

STABLE MAPS AND BRANCHED SHADOWS OF 3-MANIFOLDS

MASAHARU ISHIKAWA AND YUYA KODA

ABSTRACT. Turaev's shadow can be seen locally as the Stein factorization of a stable map. In this paper, we define the notion of stable map complexity for a compact orientable 3-manifold bounded by (possibly empty) tori counting, with some weights, the minimal number of singular fibers of codimension 2 of stable maps into the real plane, and prove that this number equals the minimal number of vertices of its branched shadows. In consequence, we give a complete characterization of hyperbolic links in the 3-sphere whose exteriors have stable map complexity 1 in terms of Dehn surgeries, and also give an observation concerning the coincidence of the stable map complexity and shadow complexity using estimations of hyperbolic volumes.

2010 Mathematics Subject Classification: 57R45; 57M27, 57N70, 58K15

Keywords: stable map; complexity; branched shadow; hyperbolic volume

INTRODUCTION

The stable maps play an important role in the study of smooth manifolds. They are especially used for obtaining topological information of the source manifold from the types of their singularities and singular fibers. A typical example is the usage of critical points of a Morse function, which is a stable map of a manifold into the real line. In this paper, we deal with stable maps from a closed orientable 3-manifold M to the real plane \mathbb{R}^2 . As is well-known, the set $S(f)$ of singular points of a stable map $f : M \rightarrow \mathbb{R}^2$ consists of *definite fold* points, *indefinite fold* points and *cusplike* points, see [23, 24]. In [23] Levine showed that the cusplike points of each stable map can be eliminated by a homotopical deformation, which implies that every 3-manifold admits a stable map into \mathbb{R}^2 without cusplike points. We note that when $f : M \rightarrow \mathbb{R}^2$ is a stable map without cusplike points, $S(f)$ forms a link in M and $f|_{S(f)}$ is an immersion with only normal crossings. A crossing of $f(S(f))$ is said to be *non-simple* if only one of the connected components of its preimage contains singularities. Burlet-de Rham [5] showed that the 3-manifolds admitting a stable map with only definite fold points are either the 3-sphere or connected sums of $S^2 \times S^1$. Saeki [36] generalized this result showing that the 3-manifolds admitting a stable map with neither non-simple crossings nor cusplike points are graph manifolds, and vice versa. It follows from Saeki's work that we need non-simple crossings to construct a stable map of a hyperbolic 3-manifold into the plane. Hence it is natural to ask how many non-simple crossings a hyperbolic 3-manifold needs to have and where is the position of

The first-named author is supported by the Grant-in-Aid for Scientific Research (C), JSPS KAKENHI Grant Number 25400078.

The second-named author is supported by Japan Society for Promotion of Science (JSPS) Postdoctoral Fellowships for Research Abroad.

the singular fibers. Costantino-Thurston [12] and Gromov [15] gave, independently, a linear lower bound of the number of non-simple crossings of stable maps that a closed 3-manifold admits in terms of Gromov norm.

On the other hand, Turaev [41, 42] introduced the notion of *shadows* of 4 and 3-manifolds in his great deal of study on quantum invariants. Roughly speaking, a shadow of a compact oriented 4-manifold W is a special kind of 2-dimensional polyhedron (*almost-special polyhedron*) P embedded in W in a locally flat way so that W collapses onto P . Then P is also called a shadow of the 3-manifold ∂W . Shadows provide a combinatorial presentation of both the 4 and 3-manifolds. In fact, by means of shadows, we can reconstruct a 4 and 3-manifold in a unique way from an almost-special polyhedron P equipped with a suitable coloring of the regions of P by half integers, which is called a *gleam*. Shadows provide important topological properties for 4 and 3-manifolds as well as being an interesting notion for the study of quantum topology. We refer the reader to Costantino-Thurston [12] for triangulations of 4 and 3-manifolds, Costantino [9, 10] for Stein structure, Spin^c structure and complex structure of 4-manifolds and Martelli [26] for a classification of 4-manifolds admitting shadows without vertices. See also the survey paper [8] by Costantino. Shadows can be defined also for a link in a compact orientable 3-manifold with (possibly empty) boundary consisting of tori. In general, shadows are defined for a trivalent graph in each compact, orientable 3-manifold, however, we consider only in the above case.

The *Stein factorization* of a map is the space of the connected components of its fibers. This is a powerful tool for the study of stable maps, because, in this case, the Stein factorization has particularly simple local shapes. In fact, in each of the papers [5], [36] and [24] mentioned earlier, Stein factorization played an important role. In [12], Costantino-Thurston revealed a strong relation between the Stein factorizations of stable maps of 3-manifolds into the plane and the shadows of the manifolds. In this paper, we study the detailed relation between *branched shadows* and stable maps of a 3-manifold (and a link in it). Here, a branched shadow is a shadow equipped with an orientation of each of their regions in a certain admissible way.

Let M be a compact, orientable 3-manifold with (possibly empty) boundary consisting of tori and L a (possibly empty) link in M . We call the minimal number of vertices in any of branched shadows of (M, L) the *branched shadow complexity* of (M, L) , and we denote it by $\text{bsc}(M, L)$. We can define another kind of complexity of (M, L) using the theory of stable maps. Here we note that the definition of stable maps can be naturally generalized for the above pair (M, L) . In this paper, we call this map an *S-map*. See Section 1.2 for details. For an S-map of (M, L) into \mathbb{R}^2 , the singular fibers over non-simple crossings are divided into two types, *types* II^2 and II^3 , according to their shapes as shown in Figure 1, see Saeki [37]. We denote by $\text{II}^2(f)$ and $\text{II}^3(f)$ the sets of singular fibers of types II^2 and II^3 , respectively, of an S-map $f : (M, L) \rightarrow \mathbb{R}^2$. We call the minimal number of the “weighted sums” $|\text{II}^2(f)| + 2|\text{II}^3(f)|$ for S-maps $f : (M, L) \rightarrow \mathbb{R}^2$ the *stable map complexity* of (M, L) , and we denote it by $\text{smc}(M, L)$. The first main result of this paper is the following:

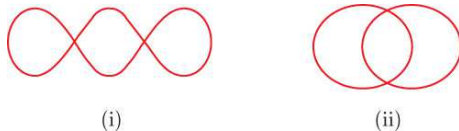


FIGURE 1. (i) A singular fiber of type II^2 ; (ii) A singular fiber of type II^3 .

Theorem 2.2. *Let M be a compact, orientable 3-manifold with (possibly empty) boundary consisting of tori and L a (possibly empty) link in M . Then we have $\text{bsc}(M, L) = \text{smc}(M, L)$.*

By Costantino-Thurston [12], the inequality $\text{sc}(M, L) \leq \text{smc}(M, L)$ holds, where $\text{sc}(M, L)$ is the *shadow complexity* of (M, L) , that is, the minimal number of vertices in any of its shadows. Since a shadow constructed from a stable map in their way is branchable, we have the inequality $\text{bsc}(M, L) \leq \text{smc}(M, L)$ immediately. To get the other inequality, we construct from a given branched shadow a stable map in 2 steps: In the first step, we construct an S-map on the submanifold of M corresponding to a neighborhood of the singularities of the branched shadow so that its Stein factorization is isomorphic to the neighborhood. In the second step, we extend this map to whole of M without creating non-simple crossings. This theorem implies branched shadows of (M, L) , which is a purely combinatorial object, determine the minimal number of the weighted sums of non-simple crossings of stable maps of (M, L) , which is a purely differential value. It is worth noting that in case where we consider a stable map of a closed orientable 3-manifold M into \mathbb{R} , instead of \mathbb{R}^2 , the minimal number of critical points is determined by some specific branched spines of M , see Remark 2.3 (3).

Due to Theorem 2.2, we can use branched shadows to study the behavior of stable map complexities under several operations of 3-manifolds. In fact, the subadditivities of branched shadow complexities under both connected sum and torus sum are obtained by easy combinatorial constructions and these provide immediately the same properties for stable map complexities (cf. Corollaries 2.6, 2.8). It follows immediately that stable map complexities do not decrease under Dehn filling (cf. Corollary 2.10). This behavior is similar to that of the hyperbolic volumes shown by Thurston [39].

In the remaining part of the paper, we discuss more applications of Theorem 2.2. First, we construct a stable map for a link in the 3-sphere using a branched shadow, and introduce a way to determine the configuration of its singular fibers. This construction and the result for Dehn filling that mentioned earlier yield the following:

Corollary 3.3. *Let M be a closed orientable 3-manifold obtained from S^3 by surgery along a link L . Then there exists a stable map $f : M \rightarrow \mathbb{R}^2$ without cusp points such that $|\text{II}^2(f)| \leq \text{cr}(L) - 2$ and $\text{II}^3(f) = \emptyset$, where $\text{cr}(L)$ is the crossing number of L .*

In [18], Kalmár-Stipsicz described the upper bounds of the minimal numbers of simple crossings, $\text{II}^2(f)$, $\text{II}^3(f)$, etc., for stable maps that a closed 3-manifold M admits in terms of properties of a surgery diagram of M . The above corollary provides better upper bounds for $|\text{II}^2(f)|$, $|\text{II}^3(f)|$ than theirs.

Next, developing the technique in the above construction, we characterize the hyperbolic knots in S^3 having branched shadow complexity 1 as follows:

Theorem 4.6. *Let L be a hyperbolic link in S^3 . Then $\text{bsc}(S^3, L) = 1$ if and only if the exterior of L is diffeomorphic to a 3-manifold obtained by Dehn filling the exterior of one of the six links L_1, L_2, \dots, L_6 in S^3 along some of (possibly none of) boundary tori of its exterior, where L_1, L_2, \dots, L_6 are illustrated in Figure 2.*

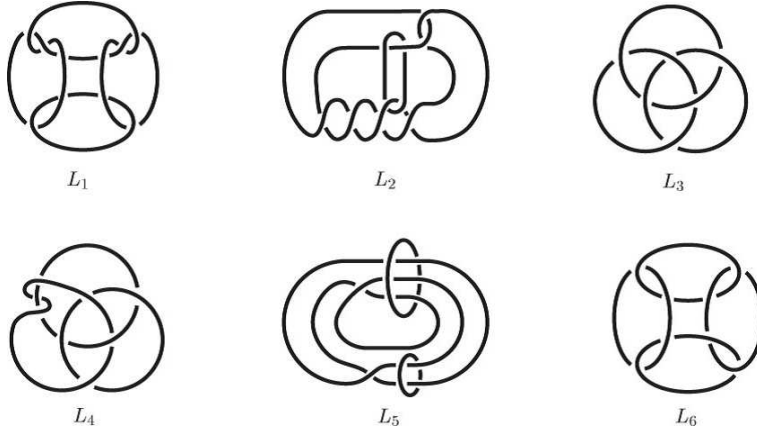


FIGURE 2. The links L_1, L_2, \dots, L_6 in S^3 .

Each of the links L_1, L_2, \dots, L_6 of this theorem is a hyperbolic link having the volume $2V_{\text{oct}}$, where $V_{\text{oct}} = 3.66\dots$ is the volume of the ideal regular octahedron. See Costantino-Thurston [12, Proposition 3.33]. We note that by Agol-Storm-Thurston [3, Theorem 9.1], the link L_1 is a minimal volume hyperbolic link that contains a meridional incompressible planar surface. See also Agol [1, Example 3.3]. In [43] Yoshida proved that the complement of L_6 is the minimal volume orientable hyperbolic 3-manifold with 4 cusps.

Theorem 4.6 can be restated in terms of singular fibers of stable maps as follows:

Corollary 4.8. *Let L be a hyperbolic link in S^3 . Then there exists a stable map $f : (S^3, L) \rightarrow \mathbb{R}^2$ without cusp points such that $|\text{II}^2(f)| = 1$ and $\text{II}^3(f) = \emptyset$ if and only if the exterior of L is diffeomorphic to a 3-manifold obtained by Dehn filling the exterior of one of the six links L_1, L_2, \dots, L_6 in Theorem 4.6 along some of (possibly none of) boundary tori of its exterior.*

We also describe the configuration of the singular fiber of the above S-map for $E(L_i)$, $i = 3, 4, 5, 6$ in Corollary 4.9.

Finally, we discuss relation between stable map complexities and hyperbolic volumes. Costantino-Thurston [12] showed the inequality $\|M\|V_{\text{tet}} \leq 2\text{sc}(M)V_{\text{oct}}$ for any 3-manifold M , where $\|M\|$ is the Gromov norm of M and $V_{\text{tet}} = 1.01\dots$ is the volume of the ideal regular tetrahedron. The same argument together with Theorem 2.2 gives the following inequality relating stable map complexities and Gromov norms:

$$\|M\|V_{\text{tet}} \leq 2\text{smc}(M)V_{\text{oct}}.$$

In particular, if M is hyperbolic then the inequality $\text{vol}(M) \leq 2 \text{smc}(M) V_{\text{Oct}}$ holds. The lower bound of $\text{vol}(M)$ by $\text{smc}(M)$ can also be given by using branched, *special* shadows, where a branched shadow P is special if P is stratified by its singularities as a CW-complex. We note that every closed orientable 3-manifold admits a branched, special shadow by the moves described in [42, 7]. By applying Futer-Kalfagianni-Purcell [14, Theorem 1.1] to our situation, we have the inequality

$$2 \text{smc}(M) V_{\text{Oct}} \left(1 - \left(\frac{2\pi}{\text{sl}(P)} \right)^2 \right)^{3/2} \leq \text{vol}(M),$$

where M is a closed orientable hyperbolic 3-manifold with special shadow P , and $\text{sl}(P)$ is a certain positive real number determined by the gleam and the topological data of P , which corresponds to the minimal slope length of Dehn fillings. We require $\text{sl}(P) > 2\pi$ in the above inequality, see Section 5 for details. From these inequalities we have the following result that concerns the coincidence of shadow complexities, branched shadow complexities and stable map complexities.

Theorem 5.2. *Let M be a closed orientable 3-manifold, and let P be a branched, special shadow of M . If $\text{sl}(P) > 2\pi\sqrt{2c(P)}$, then we have $\text{sc}(M) = \text{bsc}(M) = \text{smc}(M) = c(P)$.*

It seems to be hard to compute the shadow complexities, branched shadow complexities and stable map complexities by just looking at their definitions, because we need to consider the minimal of infinitely many shadows, branched shadows and weighted sums of non-simple crossings, respectively. Moreover, it seems to be too optimistic to expect that the shadow complexities coincide with the branched shadow complexities, since there exist infinitely many shadows that are not branchable. However, Theorem 5.2 suggests that these three kinds of complexities coincide for many cases.

This paper is organized as follows. In Section 1 we review the definitions of branched shadows and stable maps. In Section 2, we provide the proof of Theorem 2.2, and several direct corollaries of it. In Section 3, we introduce a way to construct a stable map for each link L in the 3-sphere S^3 , and describe the configuration of the fibers of the map. Section 4 is devoted to a characterization of the hyperbolic knots in S^3 having the stable map complexity 1 and its applications. In Section 5, we discuss relation between stable map complexities and hyperbolic volumes.

Throughout the paper, we will work in the smooth category unless otherwise mentioned.

1. PRELIMINARIES

1.1. Shadows and branched shadows of 3-manifolds. A compact topological space P is called an *almost-special polyhedron* if every point of P has a regular neighborhood homeomorphic to one of the five local models shown in Figure 3. A point whose regular neighborhood is shaped on the model (iii) is called a *true vertex* of P , and we denote the set of true vertices of P by $V(P)$. The set of points whose regular neighborhood are shaped on the models (ii), (iii) or (v) is called the *singular set* of P , and we denote it

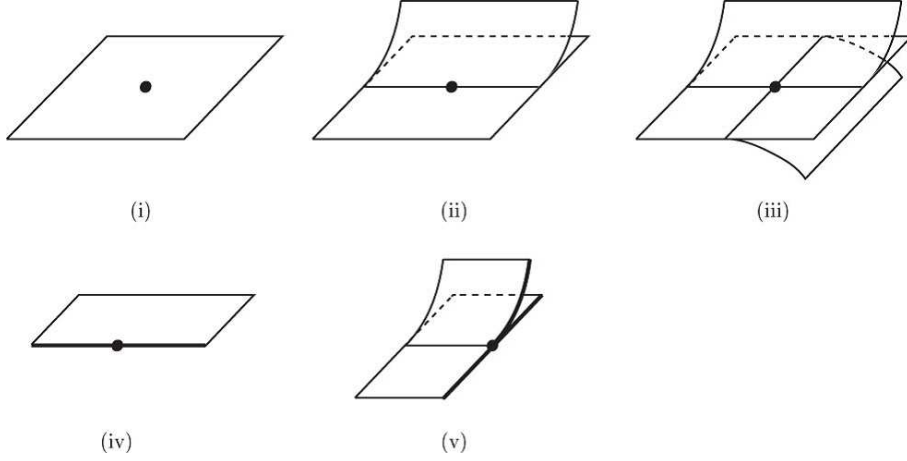


FIGURE 3. The local models of an almost-special polyhedron.

by $S(P)$. The set of points whose regular neighborhood are shaped on the models (iv) or (v) is called the *boundary* of P and we denote it by ∂P . A point whose regular neighborhood is shaped on the model (v) is called a *boundary-vertex* of P , and we denote the set of boundary-vertices of P by $BV(P)$. Throughout the paper, we set $c(P) = |V(P)| + |BV(P)|$. The polyhedron P is said to be *closed* if $\partial P = \emptyset$. Each component of $P \setminus S(P)$ is called a *region*. A region is said to be *internal* if it does not touch the boundary of P . Otherwise, it is said to be *external*.

Let P be an almost-special polyhedron. A *coloring* of ∂P is an arbitrary map from the set of components of ∂P to $\{i, e, f\}$. Then with respect to the coloring, ∂P decomposes into three peaces $\partial_i P$, $\partial_e P$ and $\partial_f P$. An almost-special polyhedron is said to be *boundary-decorated* if it is equipped with a coloring of ∂P . If $\partial_f(P) = \emptyset$, P is said to be *proper*.

Definition. Let M be a compact orientable 3-manifold and L a (possibly empty) link in M . A boundary-decorated almost-special polyhedron P properly embedded in a compact oriented smooth 4-manifold W is called a *shadow* of (M, L) if

- $W \setminus P$ is diffeomorphic to $\partial W \times (0, 1]$, or equivalently, W collapses onto P after equipping a natural PL structure on W ;
- P is locally flat, that is, each point p of P has a neighborhood $\text{Nbd}(p; P)$ that lies in a 3-dimensional submanifold of W ; and
- $(M, L) = (\partial W \setminus \text{Nbd}(\partial_e P; \partial W), \partial_i P)$.

When $L = \emptyset$, we say that P is a shadow of M for simplicity.

In [41, 42], Turaev proved that any pair of a compact orientable 3-manifold with no spherical boundary components and a (possibly empty) link in it has a shadow. In [7, 12], the *shadow complexity* of (M, L) , denoted by $\text{sc}(M, L)$, was defined to be the minimal number of true and boundary-vertices in any of its shadows.

Remark 1.1. In Costantino-Thurston [12, Remark 3.19], it is proved that, if M is a compact orientable 3-manifold with boundary consisting of (possibly empty) tori, then

$sc(M, L)$ coincides with the minimal number of true vertices in any of shadows of (M, L) . Actually, in their paper, $sc(M, L)$ was defined using only the true vertices.

A *branching* of an almost-special polyhedron P is an orientation of each region of P such that the orientations on each component of $S(P) \setminus V(P)$ induced by the regions does not coincide. A branching of P allows us to smoothen P as in the local models in Figure 3. We note that even though each region of an almost-special polyhedron P is orientable, P does not necessarily admit a branching. See Ishii [17], Benedetti-Petronio [4] and Petronio [34] for general properties of branched polyhedra.

Definition. Let M be a compact orientable 3-manifold and L a (possibly empty) link in M . A shadow P of (M, L) equipped with a branching is called a *branched shadow* of (M, L) .

In [7, Theorem 3.1.7] and [10, Proposition 3.4], Costantino described an algorithmic procedure to obtain a branched shadow from an arbitrary shadow through a finite sequence of moves. As a consequence, any pair of a compact orientable 3-manifold with no spherical boundary components and a (possibly empty) link in it has a branched shadow.

Definition. Let M be a compact orientable 3-manifold and L a (possibly empty) link in M . The *branched shadow complexity* of (M, L) , denoted by $bsc(M, L)$, is the minimal number of true and boundary-vertices in any of its branched shadows. A branched shadow P of (M, L) is said to be *minimal* if it satisfies $c(P) = bsc(M, L)$, that is, it contains the least possible number of true and boundary-vertices.

Remark 1.2. At the moment, we do not know whether $bsc(M, L)$ coincides with the minimal number of only true vertices in any of branched shadows of (M, L) if M is a compact orientable 3-manifold with boundary consisting of (possibly empty) tori. More generally, we do not know whether $sc(M, L)$ coincides with $bsc(M, L)$. See Theorem 5.2 in the last section of this paper.

A *gleam* on an almost-special polyhedron P is a coloring of all the interior regions of P with half integers satisfying a certain condition. We call an almost-special polyhedron P equipped with gleams a *shadowed polyhedron*. In [41, 42], Turaev showed the following:

- (1) If an almost-special polyhedron P is embedded in a compact oriented smooth 4-manifold W so that P is locally-flat, there exists a canonical coloring of the interior regions of P with half integers, that is, we have the canonical gleam on P .
- (2) (*Turaev's reconstruction*) From a shadowed polyhedron P , we can reconstruct a compact oriented smooth 4-manifold W and an embedding $P \hookrightarrow W$ in a unique way (up to diffeomorphism) so that W collapses onto P and the canonical gleam on P given by the embedding $P \hookrightarrow W$ coincides with the prefixed gleam on P .

Here we briefly explain the reconstruction of an oriented 4-manifold from a shadowed polyhedron P only in the case where $\partial P = \emptyset$, $S(P) \neq \emptyset$ and $S(P)$ is connected. For the detailed and general construction we refer the reader to Costantino [7] (see also Thurston [38] and Costantino-Thurston [12]). Let P be a shadowed polyhedron without boundary such that $S(P)$ is non-empty and connected. The polyhedron $\text{Nbd}(S(P); P)$ decomposes into pieces each of which is homeomorphic to a compact surface or one of

the local models (ii) and (iii) shown in Figure 3. For each piece homeomorphic to the models (ii) or (iii), we consider its 3-dimensional thickening and then glue all these pieces following a natural instruction given by the combinatorial structure of P . We note that the resulting 3-manifold X is not necessarily orientable. Let W_0 be the subbundle of the determinant line bundle over X whose fiber is $[-1, 1]$ (after giving an Euclidean metric over this bundle). This is the unique $[-1, 1]$ bundle over X whose total space is orientable. Let R be a component of $P \setminus \text{Int Nbd}(S(P); P)$. Let W_R be the subbundle of the determinant line bundle over $R \times [-1, 1]$ whose fiber is $[-1, 1]$. When R is an orientable surface, W_R is nothing else but $R \times [-1, 1] \times [-1, 1]$. The combinatorial structure of P again tells us which part of ∂W_R , which is a solid torus, will be glued to which part of ∂W_0 , which is also a torus, to obtain the required 4-manifold W .

Let l_1, l_2, \dots, l_k be k simple closed curves constituting $\partial \text{Nbd}(S(P); P) \cap R$. For each $i \in \{1, 2, \dots, k\}$, the 3-dimensional thickening of $\text{Nbd}(S(P); P)$ provides an annulus or a Möbius band B_i whose core is l_i . Similarly, the 3-dimensional thickening $R \times [-1, 1]$ provides an annulus A_i whose core is l_i . Now we have two "framings" A_i and B_i of the same simple closed curve l_i , which lie in the same solid torus after the earlier-mentioned identification. Suppose that B_i is obtained from A_i by twisting n_i times ($n_i \in (1/2)\mathbb{Z}$). See Figure 4. The gleam of the region corresponding to R is the sum $\sum_{i=1}^k n_i$.

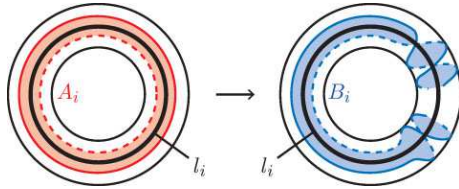


FIGURE 4. The framings A_i and B_i .

1.2. Stable maps and their Stein factorizations. Let M be a closed orientable 3-manifold. Let f be a map of M into an orientable 2-manifold Σ . We denote by $S(f)$ the set of singular points of f , that is, $S(f) = \{p \in M \mid \text{rank } df_p < 2\}$. A map f of M into Σ is said to be *stable* if there exists an open neighborhood of f in $C^\infty(M, \Sigma)$ such that for any map g in this neighborhood there exist diffeomorphisms $\Phi : M \rightarrow M$ and $\varphi : \Sigma \rightarrow \Sigma$ satisfying $g = \varphi \circ f \circ \Phi^{-1}$. Here $C^\infty(M, \Sigma)$ is the set of smooth maps of M into Σ with the Whitney C^∞ topology. If f is stable, there exist local coordinates centered at p and $f(p)$ such that f is locally described in one of the following way:

- (1) $(u, x, y) \mapsto (u, x)$;
- (2) $(u, x, y) \mapsto (u, x^2 + y^2)$;
- (3) $(u, x, y) \mapsto (u, x^2 - y^2)$;
- (4) $(u, x, y) \mapsto (u, y^2 + ux - x^3)$.

(In the cases of (1), (2), (3) and (4), p is called a *regular point*, a *definite fold point*, an *indefinite fold point* and a *cusplike point*, respectively.) Further, we require that

- (5) $f^{-1} \circ f(p) \cap S(f) = \{p\}$ for a cusplike point p ;
- (6) restriction of f to $S(f) \setminus \{\text{cusplike points}\}$ is an immersion with only normal crossings.

Conversely, if a smooth map satisfies the above conditions, then it is a stable map. The stable maps form an open dense set in the space $C^\infty(M, \Sigma)$.

Let M be a compact orientable 3-manifold with (possibly empty) boundary consisting of tori. A smooth map f of M into an orientable 2-manifold Σ is called an S -map if

- (1) the restriction of f to $\text{Int } M$ is a stable map (here a stable map means that, as in the case where M is closed, there exists an open neighborhood of f in $C^\infty(\text{Int } M, \Sigma)$ such that for any map g in this neighborhood there exist diffeomorphisms $\Phi : M \rightarrow M$ and $\varphi : \Sigma \rightarrow \Sigma$ satisfying $g = \varphi \circ f \circ \Phi^{-1}$);
- (2) for each $p \in \partial M$ there exist a local coordinate (u, x, y) centered at p , where ∂M corresponds to $\{y = 0\}$, and a local coordinate of $f(p)$ such that f is locally described as $(u, x, y) \mapsto (u, x)$.

As in Saeki [36], we denote by $S_0(f)$, $S_1(f)$ and $C(f)$ the sets of definite fold, indefinite fold, cusp points, respectively, of the restriction of f to $\text{Int } M$.

Let f be an S -map of a compact orientable 3-manifold M with (possibly empty) boundary consisting of tori into an orientable 2-manifold Σ . We say that two points p_1 and p_2 are *equivalent* if they are contained in the same component of the fibers of f . We denote by W_f the quotient space of M with respect to the equivalence relation and by q_f the quotient map. We define the map $\bar{f} : W_f \rightarrow \Sigma$ so that $f = \bar{f} \circ q_f$. The quotient space W_f , or the composition $\bar{f} \circ q_f$ is called the *Stein factorization* of f . The Stein factorization W_f is homeomorphic to a polyhedron, that is, the underlying space of a finite 2-dimensional simplicial complex.

Let f be an S -map of a compact orientable 3-manifold M with (possibly empty) boundary consisting of tori into an orientable 2-manifold Σ . By Kushner-Levine-Porto [21] and Levine [24], the local models of the Stein factorization W_f can be described as follows.

If $p \in S_0(f)$ ($p \in C(f)$, respectively), the projection $q_f(p) \mapsto f(p)$ of the Stein factorization looks locally as shown in Figure 5 (i) (Figure 5 (ii), respectively). In this case,

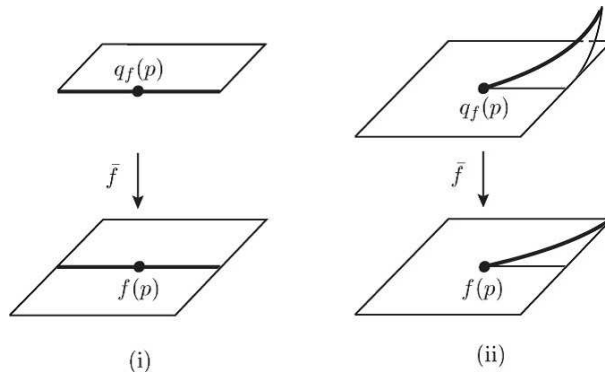


FIGURE 5. The local model of the map $\bar{f} : W_f \rightarrow \Sigma$ for: (i) a definite fold point; (ii) a cusp point.

$q_f^{-1} \circ q_f(p)$ is called a *singular fiber of type I^0* (II^a , respectively). See Saeki [37, Figure 3.4]. We remark that, in Saeki's book, these notations are defined for singular fibers of stable

maps of orientable 4-manifolds into 3-manifolds. However, the classification of singular fibers of stable maps of orientable 3-manifolds into a plane coincide with that of singular fibers of codimension 0, 1, 2 of stable maps of orientable 4-manifolds into 3-manifolds as mentioned in [37, Remark 3.14]. For this reason, we consistently use the symbols in [37, Figure 3.4] also for the remaining types of singular fibers described below.

If $p \in S_1(f)$, the projection $q_f(p) \mapsto f(p)$ looks locally as one of the three models shown in Figure 6. Let U_1, U_2 and U_3 be regular neighborhoods of points $q_f(p)$ of types

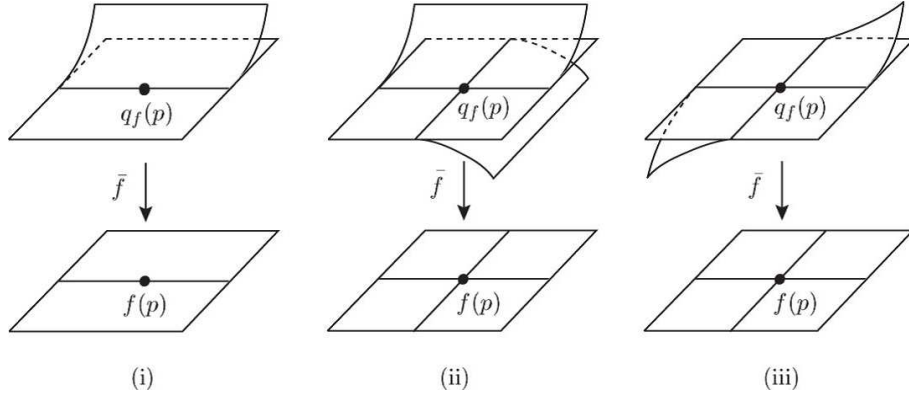


FIGURE 6. The three local models of the map $\bar{f} : W_f \rightarrow \Sigma$ for indefinite fold points.

(i), (ii) and (iii), respectively, shown in the figure. Then the preimage $q_f^{-1}(U_1) \subset M$ is diffeomorphic to $R \times [0, 1]$, where R is a pair of pants, and f maps $q_f^{-1}(U_1)$ into Σ as depicted in Figure 7. In this case $q_f^{-1} \circ q_f(p)$ is called a *singular fiber of type I^1* . Also,

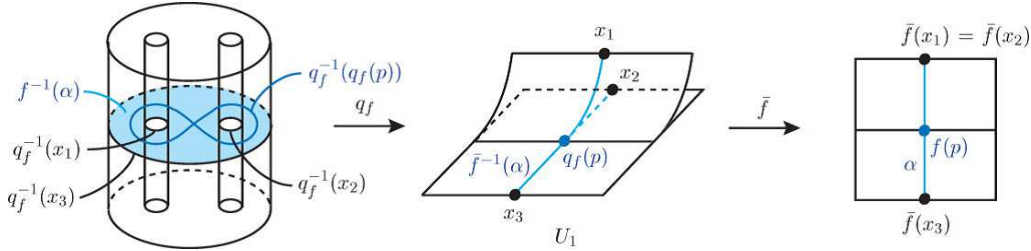


FIGURE 7. The Stein factorization of the restriction of f to $f^{-1}(U_1)$. In this figure, α is a transverse arc for f at $f(p)$. The singular fiber depicted in the figure is of Type I^1 .

the preimage $f^{-1}(U_2)$ ($f^{-1}(U_3)$, respectively) is diffeomorphic to $S \times [0, 1]$, where S is a disk with three holes, and f maps $f^{-1}(U_2)$ ($f^{-1}(U_3)$, respectively) as drawn in Figure 8 (Figure 9, respectively). In this case $q_f^{-1} \circ q_f(p)$ is called a *singular fiber of type II^2* (II^3 , respectively). We call the image in Σ of a singular fiber of type II^2 or II^3 a *non-simple*

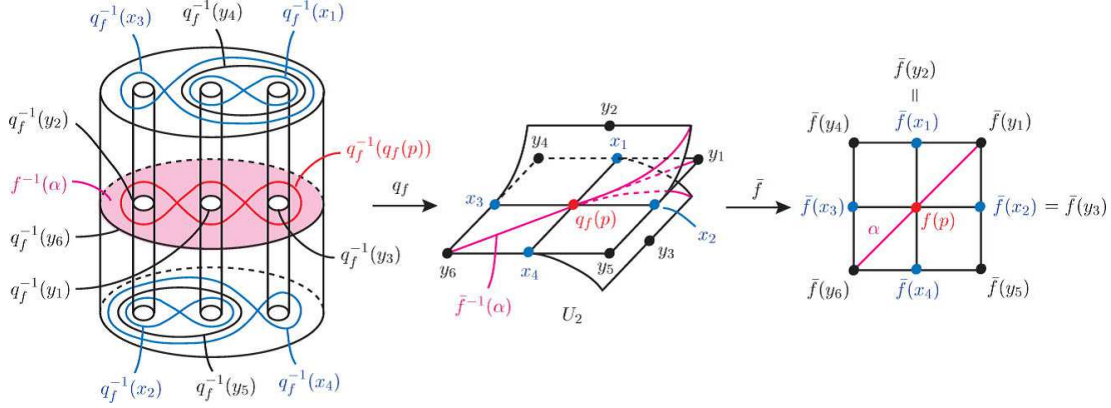


FIGURE 8. The Stein factorization of the restriction of f to $f^{-1}(U_2)$. In this figure, α is a transverse arc for f at $f(p)$. The singular fiber depicted in the figure is of Type II^2 .

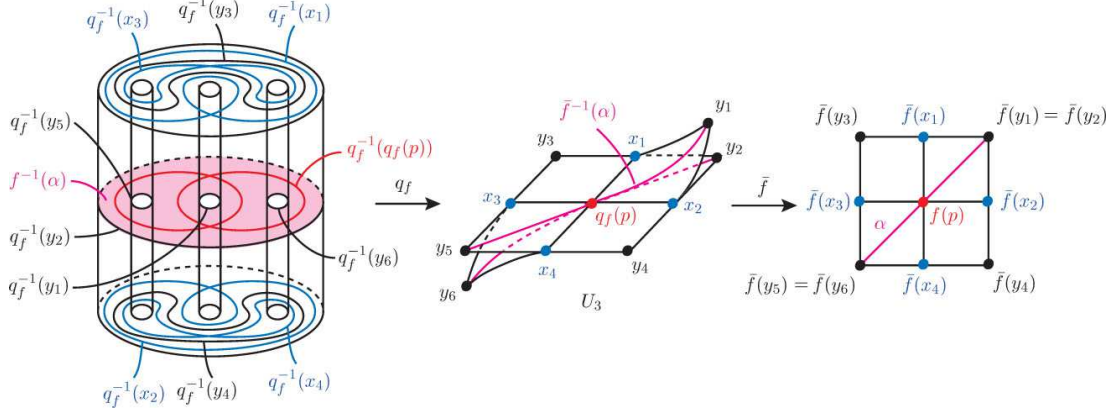


FIGURE 9. The Stein factorization of the restriction of f to $f^{-1}(U_3)$. In this figure, α is a transverse arc for f at $f(p)$. The singular fiber depicted in the figure is of Type II^3 .

crossing of f . We denote by $\text{II}^2(f)$ and $\text{II}^3(f)$ the sets of singular fibers of types II^2 and II^3 , respectively, of f .

Definition. Let M be a compact, orientable 3-manifold with (possibly empty) boundary consisting of tori and L a (possibly empty) link in M . Let $f : M \rightarrow \Sigma$ be an S-map of M into an orientable 2-manifold Σ . We say that f is an *S-map of (M, L)* (or simply of L) if $S_0(f) \supset L$. An S-map f of (M, L) is said to be *proper* if $S_0(f) = L$. When M is a closed 3-manifold, we call f a *stable map of (M, L)* .

In the following, we give several examples that will be used later. All of them appeared essentially in Saeki [36].

Example 1. We identify S^2 with $\hat{\mathbb{C}} = \mathbb{C} \cup \{\infty\}$. $D_\alpha = \{z \in \mathbb{C} \mid |z + 1/2| \leq 1/4\}$, $D_\beta = \{z \in \mathbb{C} \mid |z - 1/2| \leq 1/4\}$, $D_\gamma = \{z \in \mathbb{C} \mid |z| \geq 1\}$, $\alpha = \partial D_\alpha$, $\beta = \partial D_\beta$, $\gamma = \partial D_\gamma$.

Let $h : S^2 \rightarrow \mathbb{R}$ be a height function such that

- $h(z) = h(-z)$ for all $z \in \mathbb{C}$;
- $h(\pm 1/2) = -1$ and $h(\infty) = 1$;
- $h(\alpha) = h(\beta) = -1/2$ and $h(\gamma) = 1/2$; and
- $0 \in P$ is the unique critical point of index 1.

For each integer n , let $\rho_n : S^2 \times S^1 \rightarrow [-1, 1] \times S^1$ be the map defined by

$$\rho_n(z, \theta) = (h(z \exp(\sqrt{-1}(-n\theta/2))), \theta),$$

where we identify S^1 with $\mathbb{Z}/2\pi\mathbb{Z}$. Let $\psi : [-1, 1] \times S^1 \rightarrow \mathbb{R}^2$ be an immersion.

- (1) The map $f_n : S^2 \times S^1 \rightarrow \mathbb{R}^2$ defined by $f_n(p) = \psi \circ \rho_n(p)$ is a stable map without cusp points. For this stable map, the set $S_1(f_n)$ of indefinite fold points consists of a single circle, while the set $S_0(f_n)$ of definite fold points consists of three (two, respectively) circles when n is an even (odd, respectively) integer.
- (2) Let $f_n : S^2 \times S^1 \rightarrow \mathbb{R}^2$ be the stable map defined in (1). For each integer n , we set

$$V_n = (S^2 \times S^1) \setminus (\text{Int}(D_\gamma \times S^1) \cup \text{Int}\{(z \exp(\sqrt{-1}(n\theta/2)), \theta) \mid z \in D_\alpha \cup D_\beta\}).$$

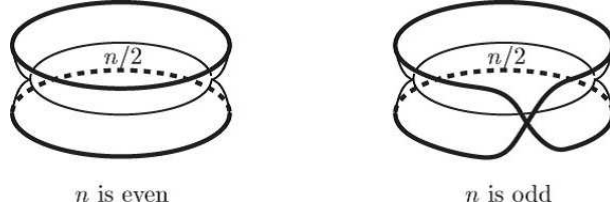
We note that V_n can be identified with $(S^2 \times S^1) \setminus \text{Int Nbd}(S_0(f_n))$. In particular, when n is an even integer, V_n is diffeomorphic to $R \times S^1$, where R is a pair of pants. The restriction of ρ_n to V_n is a map from V_n to $[-1/2, 1/2] \times S^1$. Then $f_n|_{V_n} : V_n \rightarrow \mathbb{R}^2$ is an S-map without cusp or definite fold points while the set $S_1(f_n|_{V_n})$ of indefinite fold points consists of a single circle. This map will be used in the proof of Theorem 2.2.

- (3) Set $A = \hat{\mathbb{C}} \setminus \text{Int}(D_\alpha \cup D_\beta)$ and $\rho_A = \rho_0|_{A \times S^1}$. The map $\psi \circ \rho_A : A \times S^1 \rightarrow \mathbb{R}^2$ is an S-map without cusp points. Each of $S_0(\psi \circ \rho_A)$ and $S_1(\psi \circ \rho_A)$ consists of a single circle. This map will also be used in the proof of Theorem 2.2.
- (4) Set $D = \hat{\mathbb{C}} \setminus \text{Int} D_\gamma$. The restriction of ρ_n to $D \times S^1$ is a map from $D \times S^1$ to $[-1, 1/2] \times S^1$. We identify S^3 with $(D \times S^1) \cup_\varphi (D^2 \times S^1)$, where $\varphi : \partial D^2 \times S^1 \rightarrow \partial D \times S^1$ is defined by $\varphi(\theta, \tau) = (\tau, \theta)$. Define the map $g_n : S^3 \rightarrow \mathbb{R}^2$ by

$$g_n(p) = \begin{cases} \psi_1 \circ \rho_n(p) & \text{for } p \in D \times S^1 \\ x & \text{for } p = (x, \theta) \in D^2 \times S^1 \end{cases},$$

where $\psi_1 : [-1, 1/2] \times S^1 \hookrightarrow \mathbb{R}^2 = \mathbb{C}$ is defined by $\psi_1(r, \theta) = (3/2 - r) \exp(\sqrt{-1}\theta)$ and D^2 is identified with the unit disk on \mathbb{R}^2 centered at $(0,0)$. This is a stable map without cusp points. The set $S_0(g_n)$ of definite fold points is the $(2, n)$ -torus link, in other words, g_n is a proper stable map of the $(2, n)$ -torus link. The Stein factorization W_{g_n} of this map is shown in Figure 10. We note that the almost-special polyhedron W_{g_n} equipped with the gleam $n/2$ on its disk region is a (branched) shadow of the $(2, n)$ -torus link. See Costantino-Thurston [12, Example 3.16].

Definition. Let M be a compact, orientable 3-manifold with (possibly empty) boundary consisting of tori and L a (possibly empty) link in M . Let $f : (M, L) \rightarrow \mathbb{R}^2$ be an S-map.


 FIGURE 10. The Stein Factorization W_{g_n} .

The *complexity* of f , denoted by $c(f)$, is defined by $c(f) = |\Pi^2(f)| + 2|\Pi^3(f)|$. The *stable map complexity* of (M, L) (or simply of L), denoted by $\text{smc}(M, L)$, is defined by $\text{smc}(M, L) = \min_f \{c(f)\}$, where f runs over all S-maps of (M, L) into \mathbb{R}^2 without cusp points.

Example 2. In Example 1 (4), we have seen that the stable map complexity of a $(2, n)$ -torus link is zero.

2. BRANCHED SHADOW COMPLEXITY AND STABLE MAP COMPLEXITY

Lemma 2.1. *Let M be a compact orientable 3-manifold with (possibly empty) boundary consisting of tori. Let $f : M \rightarrow S^2$ be an S-map. Then there exists an S-map $g : M \rightarrow \mathbb{R}^2$ satisfying $c(g) = |\Pi^2(f)| + 2|\Pi^3(f)|$ and $S_0(f) \subset S_0(g)$.*

Proof. The assertion follows from the construction of a stable map in Saeki [36, Lemma 3.6]. For completeness, we recall the argument.

Let $x \in S^2$ be a regular value of f . Choose two small disks D_0 and D_1 in S^2 so that $x \in D_0 \subset \text{Int } D_1$ and $f(S(f)) \cap D_1 = \emptyset$.

Let A and ρ_A be as in Example 1 (3). Let N_1, N_2, \dots, N_n be the connected components of $f^{-1}(D_1 \setminus \text{Int } D_0)$. For each $1 \leq i \leq n$, there exist diffeomorphisms $t : N_i \rightarrow A \times S^1$ and $u : [-1/2, 1] \times S^1 \rightarrow D_1 \setminus \text{Int } D_0$ such that $u \circ \rho_A \circ t = f|_{N_i}$.

Now we define the required map $g : M \rightarrow S^2 \setminus \{x\} \cong \mathbb{R}^2$ by

$$g(p) = \begin{cases} f(p) & \text{for } p \in f^{-1}(S^2 \setminus \text{Int } D_1) \\ u \circ \rho_A \circ t(p) & \text{for } p \in N_i, 1 \leq i \leq n \\ u_0 \circ f(p) & \text{for } p \in f^{-1}(D_0), \end{cases} .$$

where $u_0 : D_0 \rightarrow S^2 \setminus \{x\}$ is a smooth embedding of D_0 such that the restrictions of $u_0 \circ f$ and $u \circ \rho_A \circ t$ to $f^{-1}(D_0) \cap N_i$ coincide. Since ρ_A has no singular fibers of types Π^2 or Π^3 , g satisfies the requirement of the lemma. \square

Theorem 2.2. *Let M be a compact, orientable 3-manifold with (possibly empty) boundary consisting of tori and L a (possibly empty) link in M . Then we have $\text{bsc}(M, L) = \text{smc}(M, L)$.*

Proof. We fix an orientation of \mathbb{R}^2 .

We first prove the inequality $\text{bsc}(M, L) \leq \text{smc}(M, L)$. The argument essentially bases on the construction in the proof of Costantino-Thurston [12, Theorem 4.2]. Let $f : E(L) \rightarrow \mathbb{R}^2$ be an S-map without cusp points. Let $M \xrightarrow{q_f} W_f \xrightarrow{\tilde{f}} \mathbb{R}^2$ be the Stein

factorization of f . Then $Q = W_f \setminus \text{Int Nbd}(q_f(\text{II}^3(f)); W_f)$ is an almost-special polyhedron. We note that the number of true vertices of Q equals $|\text{II}^2(f)|$. Put $N = q_f^{-1}(Q)$. We note that $N \xrightarrow{q_f|_N} Q \xrightarrow{\bar{f}|_Q} \mathbb{R}^2$ is the Stein factorization of the map $\bar{f}|_Q \circ q_f|_N : N \rightarrow \mathbb{R}^2$. By [12], Q is a shadow of (N, L) . We may equip an orientation on each region of Q in such a way that $\bar{f}|_Q$ is locally an orientation-preserving diffeomorphism at each interior point of the region. Apparently, these orientations of the regions of Q give a branching b_0 of Q . We denote by H_1, H_2, \dots, H_n the components of $\partial Q \cap \partial \text{Nbd}(q_f(\text{II}^3(f)); W_f)$, each of which is a trivalent graph with 4 vertices. Let $N_1, N_2, \dots, N_{|\text{II}^3(f)|}$ be the components of $q_f^{-1} \text{Nbd}(q_f(\text{II}^3(f)); W_f)$, each of which is a genus 3 handlebody containing a singular fiber of type II^3 . By [12], the shadowed polyhedron Q_i shown on the left-hand side in Figure 11 is a shadow of each N_i and each component H_i of ∂Q can be capped off by Q_i so that the resulting polyhedron P is a shadow of (M, L) . We may equip a branching

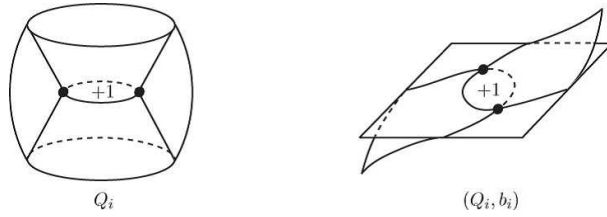


FIGURE 11. A branching of Q_i .

b_i of Q_i in such a way that the orientations on each edge of H_i induced by b_0 and b_i do not coincide, as shown on the right-hand side in Figure 11. Then the branchings b_0 and b_i give a branching of P . It is straightforward from the above construction that the number of the true vertices of P is $|\text{II}^2(f)| + 2|\text{II}^3(f)|$ while P has no boundary-vertices, so we are done.

In the following we will show the other inequality: $\text{bsc}(M, L) \geq \text{smc}(M, L)$. Let $P \subset W$ be a minimal branched shadow of (M, L) . By Lemma 2.1, it suffices to show that there exists an S-map $f : E(L) \rightarrow S^2$ satisfying $|\text{II}^2(f)| + 2|\text{II}^3(f)| = \text{bsc}(M, L)$. Suppose that P contains non-empty boundary-vertices. Let G_1, G_2, \dots, G_n be the components of $\partial_f P$ containing at least one boundary vertex. For each $1 \leq i \leq n$, let F_i be a compact orientable surface such that there exists an embedding $\iota_i : G_i \rightarrow \text{Int } F_i$ and F_i collapses onto $\iota_i(G_i)$. Fix an orientation of F_i in an arbitrary way. We attach P to each F_i by the map ι_i and we denote the resulting polyhedron by P^* . The branching of P and the orientations of F_1, F_2, \dots, F_n give a branching of P^* . See Figure 12. We note that by this operation, each boundary-vertex of P gives rise to a true vertex of P^* and no other true or boundary-vertices are produced. Thus P^* has no boundary-vertices and we have $|V(P^*)| = c(P) = \text{bsc}(M, L)$. Therefore we may assume without loss of generality that P has no boundary-vertices.

We choose a collapsing $W \searrow P$ so that the induced projection $\pi : M \rightarrow P$ satisfies the following:

- for each $x \in \partial P$, $\pi^{-1}(p)$ is a single point;

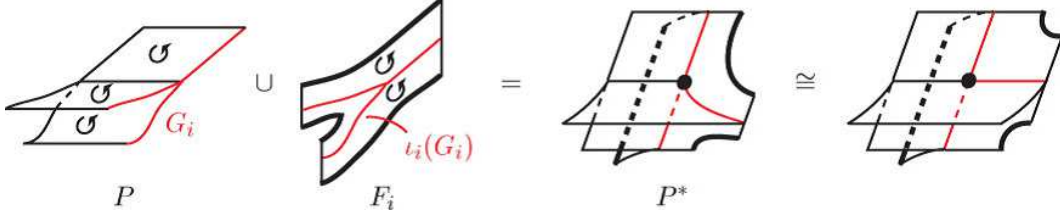
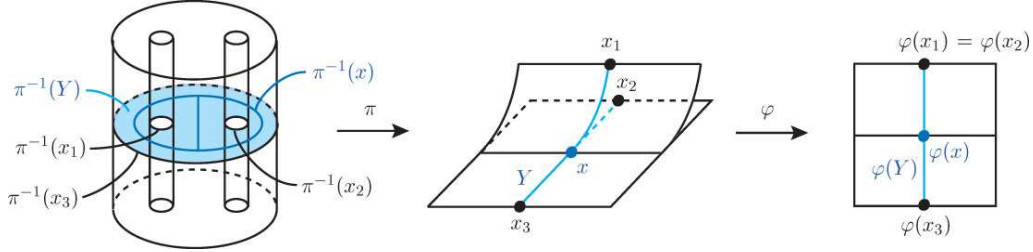


FIGURE 12. Elimination of boundary-vertices.

- for each $x \in V(P)$, $\pi^{-1}(x) \cong T_4$, where T_4 is the suspension of four points;
- for each $x \in S(P) \setminus V(P)$, $\pi^{-1}(x) \cong T_3$, where T_3 is the suspension of three points; and
- the restriction of π to the preimage $\pi^{-1}(P \setminus (\partial P \cup S(P)))$ is a trivial, smooth S^1 -bundle.

Note that for the construction of the projection π , we do not need a branching of P . For a point x in $S(P) \setminus V(P)$, the preimage of $\text{Nbd}(x)$ under π is diffeomorphic to $R \times [0, 1]$, where R is a pair of pants, and π is described as on the left-hand side in Figure 13. Also,


 FIGURE 13. The local model of π and φ for $\text{Nbd}(x; P)$, where $x \in S(P) \setminus V(P)$.

for a point x in $V(P)$, the preimage of $\text{Nbd}(x)$ under π is diffeomorphic to $S \times [0, 1]$, where S is a disk with 3 holes, and π is described as on the left-hand side in Figure 14.

Let v_1, v_2, \dots, v_{n_0} be the true vertices of P . We put

$$P' = P \setminus \left(\text{Nbd}(\partial P; P) \cup \left(\bigcup_{i=1}^{n_0} \text{Nbd}(v_i; P) \right) \right).$$

The set of components of $S(P')$ consists of intervals e_1, e_2, \dots, e_{m_1} and circles l_1, l_2, \dots, l_{n_1} . We note that $\text{Nbd}(e_i; P')$ is homeomorphic to $Y \times [0, 1]$, and $\text{Nbd}(l_j; P')$ is homeomorphic to $Y \times S^1$ or $Y \times [0, 2\pi]/(z, 2\pi) \sim (\rho(z), 0)$, where Y is a Y-shaped graph that we identify with $Y = \{r \exp(\sqrt{-1}\theta) \in \mathbb{C} \mid 0 \leq r \leq 1, \theta = 0 \text{ or } \pm 2\pi/3\}$ and $\rho : Y \rightarrow Y$ is defined by the complex conjugation. With this homeomorphisms, we equip each of $\text{Nbd}(e_i; P')$ and $\text{Nbd}(l_j; P')$ with a Y -bundle structure. In the following, we put the three boundary points of Y as $a = \exp((\sqrt{-1})2/3\pi)$, $b = \exp((\sqrt{-1})(-2/3\pi))$ and $c = 1$. The set of

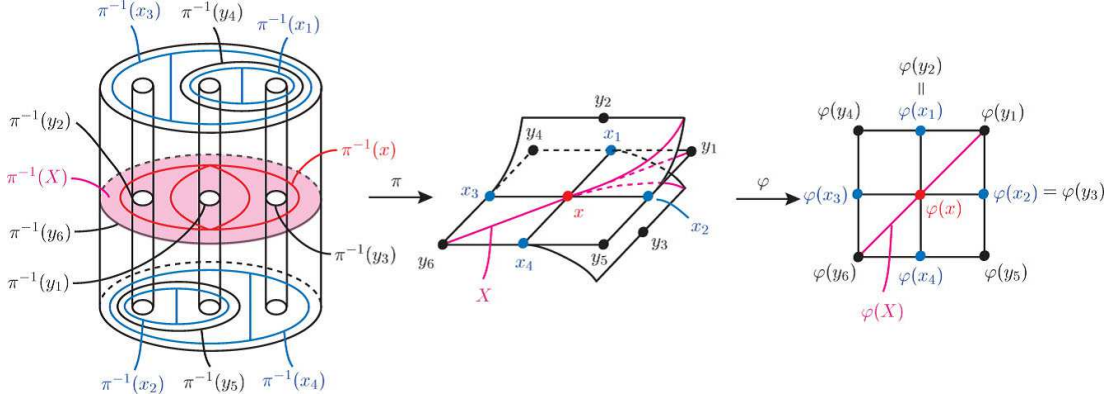


FIGURE 14. The local model of π and φ for $\text{Nbd}(x; P)$, where $x \in V(P)$.

components of

$$P' \setminus \left(\left(\bigcup_{i=1}^{m_1} \text{Nbd}(e_i; P') \right) \cup \left(\bigcup_{i=1}^{n_1} \text{Nbd}(l_i; P') \right) \right) = P \setminus \text{Int Nbd}(\partial P \cup S(P); P)$$

consists of oriented surfaces R_1, R_2, \dots, R_{n_2} .

We set $N = \pi^{-1}(\text{Nbd}(\partial P \cup S(P); P))$. Since $\text{Nbd}(\partial P \cup S(P); P)$ is a branched polyhedron, there exists a map $\varphi : \text{Nbd}(\partial P \cup S(P); P) \rightarrow S^2$ satisfying the following (see the right-hand side in Figures 13 and 14):

- φ is generic on $S(P)$, that is, φ is an injection on $S(P)$ except at finitely many double points, which are the projections of only two points of $S(P) \setminus V(P)$ and at the crossing points the two threads project to two different directions on S^2 ;
- For $1 \leq i < j \leq n_0$, $\varphi(\partial \text{Nbd}(v_i)) \cong S^1$ and $\varphi(\text{Nbd}(v_i)) \cap \varphi(\text{Nbd}(v_j)) = \emptyset$;
- φ is locally an orientation-preserving diffeomorphism at each point of $\text{Nbd}(\partial P \cup S(P); P) \setminus S(P)$;
- $\varphi(\text{Nbd}(S(P); P))$ is a regular neighborhood of $\varphi(S(P))$ in S^2 ;
- for each $x \in e_i$ ($x \in l_i$, respectively), the fiber Y_x of the Y -bundle structure of $\text{Nbd}(e_i; P')$ ($\text{Nbd}(l_i; P')$, respectively) is mapped into a segment by $re^{i\theta} \mapsto r \cos \theta$.

Claim 1. *There exists an S -map $g : N \rightarrow S^2$ with the Stein factorization $N \xrightarrow{q_g} W_g \xrightarrow{\bar{g}} S^2$ such that*

- $g(N) = \varphi \circ \pi(N)$;
- $W_g \cong \text{Nbd}(\partial P \cup S(P); P)$; and
- the following diagram commutes:

$$\begin{array}{ccc} \partial N & \xrightarrow{q_g} & W_g \\ \pi \downarrow & \circlearrowleft & \downarrow \bar{g} \\ \text{Nbd}(\partial P \cup S(P); P) & \xrightarrow{\varphi} & S^2 \end{array}$$

Proof of Claim 1. It is clear from the local model of the definite fold points (recall Figure 5 (i)) and the definition of φ that $\pi^{-1}(\text{Nbd}(\partial P; P))$ consists of finitely many solid tori and there exists an S-map $g_{\partial P} : \pi^{-1}(\text{Nbd}(\partial P; P)) \rightarrow S^2$ with the Stein factorization $\pi^{-1}(\text{Nbd}(\partial P; P)) \xrightarrow{q_{g_{\partial P}}} W_{g_{\partial P}} \xrightarrow{\bar{g}_{\partial P}} S^2$ such that

- $g_{\partial P}(\pi^{-1}(\text{Nbd}(\partial P; P))) = \varphi(\text{Nbd}(\partial P; P))$;
- $W_{g_{\partial P}} \cong \text{Nbd}(\partial P; P)$; and
- $\bar{g}_{\partial P} \circ q_{g_{\partial P}} = \varphi \circ \pi$ on $\partial\pi^{-1}(\text{Nbd}(\partial P; P))$.

For each $1 \leq i \leq n_1$, we identify $\text{Nbd}(l_i; P)$ with $Y \times S^1$ or $Y \times [0, 2\pi]/(z, 2\pi) \sim (\rho(z), 0)$ as mentioned earlier. Here we identify them so that the points $(a, 0) \in Y \times S^1$ and $(b, 0) \in Y \times S^1$ lie on the regions of P that induce the same orientation on l_i . The map $\varphi|_{\text{Nbd}(l_i; P)} : \text{Nbd}(l_i; P) \rightarrow S^2$ factors through $\text{Nbd}(l_i; P) \xrightarrow{\varphi_1} [-1/2, 1/2] \times S^1 \xrightarrow{\varphi_2} S^2$, where φ_1 is defined by $\varphi_1(r \exp(\sqrt{-1}(\pm 2\pi/3))) = -r/2$ and $\varphi_1(r) = r/2$ for $0 \leq r \leq 1$. For $n \in \mathbb{Z}$, let V_n and ρ_n be as defined in Example 1 (2). Then by construction, we may identify $\pi^{-1}(Y \times S^1)$ with V_0 or V_1 , depending on whether $\text{Nbd}(l_i; P)$ is $Y \times S^1$ or $Y \times [0, 2\pi]/(\rho(z), 2\pi) \sim (z, 0)$, so that $\varphi_2 \circ \rho_n$ coincides with $\varphi \circ \pi|_{V_n}$ on ∂V_n . We denote the map $\varphi_2 \circ \rho_n : \pi^{-1}(\text{Nbd}(l_i; P)) \rightarrow S^2$ by g_{l_i} .

For each $1 \leq j \leq m_1$, we identify $\text{Nbd}(e_j; P')$ with $Y \times [0, 1]$. As in the above argument, we may assume that the points $(a, 0) \in Y \times S^1$ and $(b, 0) \in Y \times S^1$ lie on the regions of P that induce the same orientation on e_j . The map $\varphi|_{\text{Nbd}(e_j; P')} : \text{Nbd}(e_j; P') \rightarrow S^2$ factors through $\text{Nbd}(e_j; P') \xrightarrow{\varphi_1} [-1/2, 1/2] \times [0, 1] \xrightarrow{\varphi_2} S^2$, where φ_1 is defined by $\varphi_1(r \exp(\sqrt{-1}(\pm 2\pi/3))) = -r/2$ and $\varphi_1(r) = r/2$ for $0 \leq r \leq 1$. Let $R = \hat{\mathbb{C}} \setminus \text{Int}(D_\alpha \cup D_\beta \cup D_\gamma)$ and $\rho_0 : R \times S^1 \rightarrow [-1/2, 1/2]$ be as in Example 1 (2). By construction, we may identify $\pi^{-1}(Y \times [0, 1])$ with $R \times [0, 1]$ so that $\varphi_2 \circ \rho_0|_{R \times [0, 1]}$ coincides with $\varphi \circ \pi|_{R \times [0, 1]}$ on $\partial R \times [0, 1]$. We denote the map $\varphi_2 \circ \rho_0|_{R \times [0, 1]} : \pi^{-1}(\text{Nbd}(e_j; P')) \rightarrow S^2$ by g_{e_j} .

Finally, for each $1 \leq k \leq n_0$, we identify $\pi^{-1}(\text{Nbd}(v_k; P))$ with $S \times [0, 1]$ as shown in Figure 14, where we recall that S is a disk with 3 holes. Let $g_{v_k} : S \times [0, 1] \rightarrow S^2$ be the local model of an S-map in a small neighborhood of a singular fiber of type II² shown in Figure 8 with the Stein factorization $S \times [0, 1] \xrightarrow{q_{g_{v_k}}} W_{g_{v_k}} \xrightarrow{\bar{g}_{v_k}} S^2$ such that

- $g_{v_k}|_{\partial S \times [0, 1]} = \varphi \circ \pi|_{\partial S \times [0, 1]}$;
- $g_{v_k}(S \times \{t\}) = \varphi \circ \pi(S \times \{t\})$; and
- the Stein factorization $W_{g_{v_k}}$ is isomorphic to $\text{Nbd}(v_k; P)$ as branched polyhedron, where we equip an orientation of each region of $W_{g_{v_k}}$ in such a way that map \bar{g}_{v_k} is locally an orientation-preserving diffeomorphism on the region.

Since P is equipped with a branching, a small C^∞ -perturbation allows us to assume that, on each component of $\pi^{-1}(\text{Nbd}(v_k; P) \cap \text{Nbd}(e_j; P'))$, that is a pair of pants, g_{v_k} and g_{e_j} coincide.

Now, we define a map $g : N \rightarrow S^2$ by

$$g(p) = \begin{cases} g_{\partial P}(p) & \text{for } p \in \pi^{-1}(\text{Nbd}(\partial P; P)); \\ g_{l_i}(p) & \text{for } p \in \pi^{-1}(\text{Nbd}(l_i; P')), 1 \leq i \leq n_1; \\ g_{e_j}(p) & \text{for } p \in \pi^{-1}(\text{Nbd}(e_j; P')), 1 \leq j \leq m_1; \\ g_{v_k}(p) & \text{for } p \in \pi^{-1}(\text{Nbd}(v_k; P)), 1 \leq k \leq n_0. \end{cases}$$

This completes the proof of the claim. \square

By the above claim, it suffices to show that, for each $1 \leq i \leq n_2$, there exists an S-map $g_{R_i} : \pi^{-1}(R_i) \rightarrow S^2$ such that

- $g_{R_i}|_{\partial(\pi^{-1}(R_i))} = g|_{\partial(\pi^{-1}(R_i))}$; and
- g_{R_i} admits no singular fibers of types II^2 or II^3 .

First we prove the assertion in the case where each surface R_i is a disk for each $i \in \{1, 2, \dots, n_2\}$. We fix the index i and prove the existence of such an S-map of $\pi^{-1}(R_i)$. Hereafter we identify $\pi^{-1}(R_i)$ with $R_i \times S^1$. By small perturbation of the map g , we may assume that $\bar{g}(\partial R_i)$ has only normal double points. Choose a smooth arc in $\bar{g}(\partial R_i)$ which starts and ends at the same point, i.e., a double point of $\bar{g}(\partial R_i)$, and has no other double points. Such a smooth arc can be found by choosing a suitable double point. Choose a band $b_1 = [0, 1] \times [0, 1]$ in R_i with $\text{Nbd}(S(P); P) \cap b_1 = \{0, 1\} \times [0, 1]$ and a map $\bar{g}_{b_1} : \text{Nbd}(S(P); P) \cup b_1 \rightarrow S^2$ such that $\bar{g}_{b_1}|_{\text{Nbd}(S(P); P)} = \bar{g}$ and the image $\bar{g}_{b_1}(b_1)$ of b_1 is as shown in Figure 15. This map induces an S-map $g_{b_1} : N \cup (b_1 \times S^1) \rightarrow S^2$

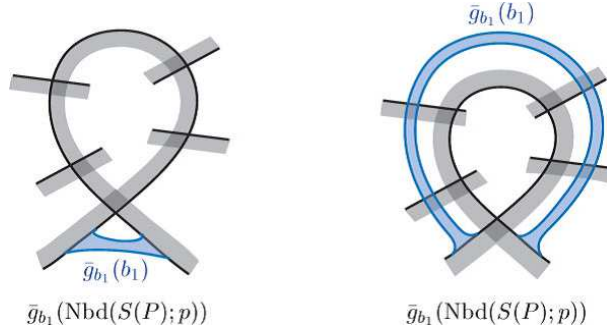


FIGURE 15. Extension of \bar{g} over a band b_1 .

satisfying

- $g_{b_1}|_N = g$; and
- the Stein factorization of g_{b_1} is given as $g_{b_1} = \bar{g}_{b_1} \circ q_{g_{b_1}}$, where $q_{g_{b_1}}|_{b_1 \times S^1} : b_1 \times S^1 \rightarrow b_1$ is the first projection.

Note that $b_1 \times S^1 \subset R_i \times S^1$ and $b_1 \times S^1$ is attached to N according to the identification of $\pi^{-1}(R_i)$ with $R_i \times S^1$. Since R_i is a disk, the closure of $R_i \setminus b_1$ consists of two disjoint disks, say R'_i and R''_i , such that

- $\bar{g}_{b_1}(\partial R'_i)$ has just one double point; and
- the number of double points of $\bar{g}_{b_1}(\partial R''_i)$ is less than that of $\bar{g}(\partial R_i)$.

Next, we choose the surface R''_i and apply the same argument, i.e., attach a band b_2 and make an S-map $g_{b_2} : N \cup (b_1 \times S^1) \cup (b_2 \times S^1) \rightarrow S^2$. We continue this process successively until $\bar{g}_{b_j}(c)$ has at most one double point for each boundary component c of the closure of $R_i \setminus (b_1 \cup \dots \cup b_j)$. Since the number of double point of $\bar{g}(\partial R_i)$ is finite this process ends at a finite number of steps, say n_3 steps. As a consequence, we obtain an S-map $g_B : N \cup (B \times S^1) \rightarrow S^2$, where $B = \cup_{j=1}^{n_3} b_j$, such that

- $g_B|_N = g$;
- the Stein factorization of g_B is given as $g_B = \bar{g}_B \circ q_{g_B}$, where $\bar{g}_B = \bar{g}_{b_{n_3}}$ and $q_{g_B}|_{B \times S^1} : B \times S^1 \rightarrow B$ is the first projection; and
- for each boundary component c of the closure of $R_i \setminus B$, $\bar{g}_B|_c$ is an immersion of a circle into S^2 such that it has at most one double point.

Suppose that c_0 is a boundary component of the closure of $R_i \setminus B$ such that $\bar{g}_B(c_0)$ has no double point and let D_{c_0} denote the disk in R_i bounded by c_0 . In this case, the S-map $g_{c_0} : N \cup (B \times S^1) \cup (D_{c_0} \times S^1) \rightarrow S^2$ is easily obtained by choosing the image $\bar{g}_{c_0}(D_{c_0})$ to be the disk bounded by $\bar{g}_B(c_0)$, where $N \cup (B \times S^1) \cup (D_{c_0} \times S^1) \subset M$ due to the identification of $\pi^{-1}(R_i)$ with $R_i \times S^1$.

Suppose that c_1 is a boundary component of the closure of $R_i \setminus B$ such that $\bar{g}_B(c_1)$ has exactly one double point. Let V_1 and $f_1|_{V_1} : V_1 \rightarrow \mathbb{R}^2$ be as in Example 1 (2). We regard V_1 as the exterior of an open tubular neighborhood of a $(2, 1)$ -cable knot in the solid torus $D^2 \times S^1$ and set $T = \partial(D^2 \times S^1)$ and $T_1 = \partial V_1 \setminus T$. Let $\phi : V_1 \rightarrow V_1$ be an orientation-preserving diffeomorphism such that the positions of two boundary tori exchange, and set $f_\phi = f_1|_{V_1} \circ \phi$. The image $f_\phi(V_1)$ is an annulus in \mathbb{R}^2 . If the preimage of a point on the boundary of $f_\phi(V_1)$ is on T then it is $\{a_1, a_2\} \times S^1$, where a_1, a_2 are distinct two points on ∂D^2 . If the preimage is on T_1 , then it is a longitude of the $(2, 1)$ -cable knot.

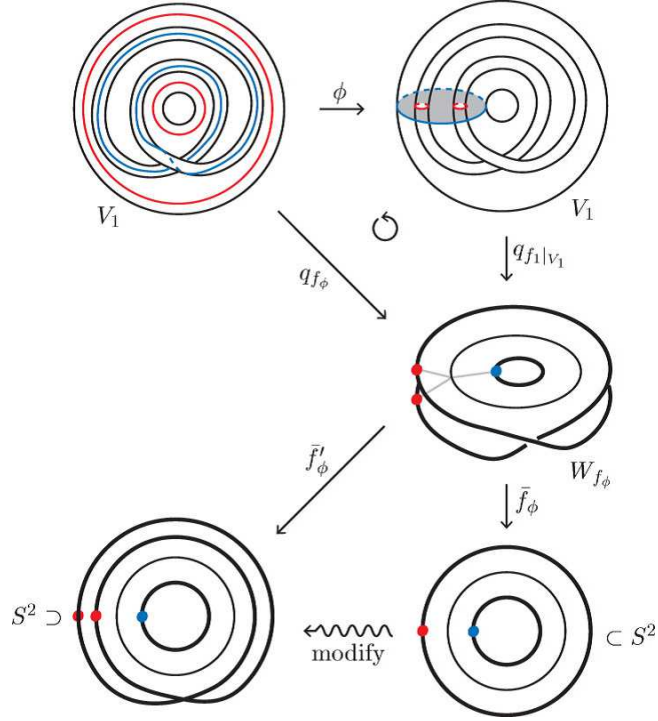
Consider the Stein factorization of f_ϕ , i.e., $V_1 \xrightarrow{q_{f_\phi}} W_{f_\phi} \xrightarrow{\bar{f}_\phi} S^2$. Attach W_{f_ϕ} to $\text{Nbd}(S(P); P) \cup B$ smoothly so that $(\text{Nbd}(S(P); P) \cup B) \cap W_{f_\phi} = q_{f_\phi}(T) = c_1$, and then attach V_1 to $N \cup (B \times S^1)$ so that $q_{f_\phi}|_T = g_B|_T$. Here the solid torus $D^2 \times S^1$ including V_1 is identified with $\pi^{-1}(D_{c_1}) \subset \pi^{-1}(R_i)$, where D_{c_1} is the disk in R_i bounded by c_1 . We need to modify the map f_ϕ to f'_ϕ , with keeping $q_{f_\phi} = q_{f'_\phi}$, so that $\bar{f}'_\phi|_{q_{f'_\phi}(T)} = \bar{g}_B|_{c_1}$. In other words, modify it in such a way that the S-map $g_{c_1} : N \cup (B \times S^1) \cup V_1 \rightarrow S^2$ defined by

$$g_{c_1} = \begin{cases} g_B(p) & \text{for } p \in N \cup (B \times S^1) \\ f'_\phi(p) & \text{for } p \in V_1 \end{cases}$$

is well-defined. The existence of such a modification of f_ϕ can be checked as follows: We set $N_{c_1} = \text{Nbd}(c_1; \text{Nbd}(S(P); P) \cup B)$, which is an annulus. The image $\bar{g}_B(N_{c_1})$ is an immersed annulus such that the image of one of the immersed boundary components is $\bar{g}_B(c_1)$. There are two regions in $S^2 \setminus \text{Int } \bar{g}_B(N_{c_1})$ which have just one corner, and one of these regions is bounded by $\bar{g}_B(c_1)$. Taking the image of f_ϕ in this region, we see that f_ϕ can be modified so that it coincides with $\bar{g}_B|_{c_1}$ on $q_{f_\phi}(T)$. See Figure 16.

We attach a solid torus to V_1 along the boundary torus T_1 as follows: We first recall the construction of the map $h_2 : T^2 \times [0, 1] \rightarrow \mathbb{R}^2$ given in Saeki [36, p. 680], where T^2 is a torus. Let R be a pair of pants and a be one of its boundary components. Let $\chi : \partial D^2 \times S^1 \rightarrow a \times S^1$ be the diffeomorphism defined by $\chi(\theta, \tau) = (\theta + \tau, \tau)$ and set $X = (R \times S^1) \cup_\chi (D^2 \times S^1)$, which is diffeomorphic to $T^2 \times [0, 1]$. Then define $h_2 : T^2 \times [0, 1] \rightarrow \mathbb{R}^2$ by

$$h_2(p) = \begin{cases} (h(p_1), p_2) \in \mathbb{R} \times S^1 \subset \mathbb{R}^2 & \text{for } p = (p_1, p_2) \in R \times S^1 \\ q_1 \in D^2 \subset \mathbb{R}^2 & \text{for } p = (q_1, q_2) \in D^2 \times S^1, \end{cases}$$

FIGURE 16. Extension of g_B over D_{c_1} .

where $h : R \rightarrow \mathbb{R}$ is the Morse function as in Example 1 with regarding that R is the pair of pants bounded by α, β and γ . The map h_2 has the following important property: For $i = 0, 1$, let $\mu_i \subset T^2 \times \{i\}$ be a section of $h \times \text{id}_{S^1} : R \times S^1 \rightarrow \mathbb{R} \times S^1$ and λ_i be a fiber of h_2 on $T^2 \times \{i\}$. Then h_2 satisfies $[\lambda_0] = [\mu_1]$ and $[\mu_0] = [\lambda_1]$ in $H_1(T^2 \times [0, 1])$.

Set $U = \text{Nbd}(T_1; V_1)$ and $T_0 = \partial U \setminus T_1$. Let D denote the disk in S^2 bounded by the simple closed curve $g_{c_1}(T_0)$. There exist diffeomorphisms $t : U \rightarrow T^2 \times [0, 1]$ and $u : D^2 \rightarrow D \subset S^2$ such that $u \circ h_2 \circ t|_{T_0} = g_{c_1}|_{T_0}$. Then we define an S-map $g'_{c_1} : N \cup (B \times S^1) \cup V_1 \rightarrow S^2$ by

$$g'_{c_1} = \begin{cases} g_{c_1}(p) & \text{for } p \in N \cup (B \times S^1) \cup V_1 \setminus (\text{Int } U \cup T_1) \\ u \circ h_2 \circ t(p) & \text{for } p \in U. \end{cases}$$

Since each fiber of the map g'_{c_1} on T_0 is a longitude, the fiber of g'_{c_1} on T_1 is the meridian of the $(2, 1)$ -cable knot. The compact tubular neighborhood of an S^1 -family of definite fold points is a solid torus whose fiber on the boundary is the meridian. Attaching this solid torus to $N \cup (B \times S^1) \cup V_1$ along T_1 , we obtain the S-map from $N \cup (B \times S^1) \cup (D^2 \times S^1)$ to S^2 , where $D^2 \times S^1$ is the solid torus obtained from V_1 by filling the boundary T_1 canonically.

We apply the same construction for all boundary components of the closure of $R_i \setminus B$ and obtain an S-map $g_{C_i} : N \cup (R_i \times S^1) \rightarrow S^2$.

Applying this construction to all surfaces R_1, \dots, R_{n_2} , we obtain the S-map $g_C : M \rightarrow S^2$ with the required properties. This completes the proof in the case where each surface R_i is a disk.

Suppose that some of R_1, \dots, R_{n_2} is not a disk. Let Γ be the union of mutually disjoint, essential simple closed curves in $R_1 \cup \dots \cup R_{n_2}$ that cuts $R_1 \cup \dots \cup R_{n_2}$ into planar surfaces each of which contains at most one boundary component of $\text{Nbd}(\partial P \cup S(P); P)$. We remark that the polyhedron P cut off by Γ may not be connected. We denote by \hat{P} the almost-special branched polyhedron obtained by cutting P along Γ and then capping off the new boundary components by disks. Let \hat{M} be the 3-manifold represented by \hat{P} after giving suitable gleams to the new disk regions. Since each region of \hat{P} is a disk, by applying the above argument, we obtain an S-map $g_C : \hat{M} \rightarrow S^2$. To recover P , we first remove suitable number of disks from the regions of \hat{P} and also remove their preimages in \hat{M} . We assume that the removed disks are near the boundary of $\text{Nbd}(S(P); P)$ and it is sufficiently small so that their images in S^2 have no intersection.

Let D_0 and D_1 be disks in \hat{P} whose boundaries will be identified. Set $A_j = \text{Nbd}(\partial D_j; \hat{P} \setminus \text{Int } D_j)$ for $j = 0, 1$. The preimage $q_{g_C}^{-1}(A_j)$ has two boundary components, one of which is $q_{g_C}^{-1}(\partial D_j)$ named $T_{j,1}$. We denote the other boundary component by $T_{j,0}$. Let A and ρ_0 be as in Example 1 (3). For each $j = 0, 1$, there exist diffeomorphisms $t_j : q_{g_C}^{-1}(A_j) \rightarrow A \times S^1$ and $u_j : [-1/2, 1] \times S^1 \rightarrow \bar{g}_C(A_j)$ such that $u_j \circ \rho_0 \circ t_j|_{T_{j,0}} = g_C|_{T_{j,0}}$. Then we define an S-map $g_D : \hat{M} \setminus q_{g_C}^{-1}(\text{Int}(D_0 \cup D_1)) \rightarrow S^2$ by

$$g_D(p) = \begin{cases} g_C(p) & \text{for } p \notin q_{g_C}^{-1}(A_j \cup D_j) \\ u_j \circ \rho_0 \circ t_j(p) & \text{for } p \in q_{g_C}^{-1}(A_j). \end{cases}$$

Remark that $g_D(T_{0,1})$ and $g_D(T_{1,1})$ are simple closed curves in S^2 and the interior of the annulus bounded by these curves does not intersect $g_D(A_j)$ for $j = 0, 1$. We attach an annulus A_2 between ∂D_0 and ∂D_1 and define the S-map $g'_D : M' \rightarrow S^2$ with Stein factorization $M' \xrightarrow{q_{g'_D}} W_{g'_D} \xrightarrow{\bar{g}'_D} S^2$ such that $\bar{g}'_D(A_2)$ is the annulus bounded by $g_D(T_{0,1})$ and $g_D(T_{1,1})$, where $M' = (\hat{M} \setminus q_{g_C}^{-1}(\text{Int}(D_0 \cup D_1))) \cup (A_2 \times S^1)$. Applying this construction for each pair of disks in \hat{P} whose boundary should be identified, and adjusting the gleam by removing and re-gluing a compact neighborhood of the fiber of a point in ∂R_i with keeping the existence of an S-map, we obtain the S-map $g_E : M \rightarrow S^2$ with the required properties. This completes the proof. \square

Remark 2.3. (1) Let (M, L) be as in Theorem 2.2, and let $f : (M, L) \rightarrow \mathbb{R}^2$ be an S-map. If $\text{II}^3(f) = \emptyset$, the Stein factorization W_f is exactly a branched shadow of (M, L) . Suppose that $\text{II}^3(f) \neq \emptyset$, and let N_1, N_2, \dots, N_n be closed neighborhoods of the singular fibers of type II^3 . We recall that each N_i is a genus 3 handlebody. By the latter part of the proof of Theorem 2.2, we may construct a map $g_i : N_i \rightarrow \mathbb{R}^2$ using the shadowed branched polyhedron depicted in Figure 11. Exchanging f with g_i inside N_i for each $i \in \{1, 2, \dots, n\}$, we get a new S-map $(M, L) \rightarrow \mathbb{R}^2$ having no singular fibers of type II^3 .

(2) Let (M, L) be as in Theorem 2.2 and let P be its branched shadow having no boundary-vertices. By the latter part of the proof of Theorem 2.2, we may

construct an S-map $f : E(L) \rightarrow \mathbb{R}^2$ with $|\text{II}^2(f)| = c(P)$ and $\text{II}^3(f) = \emptyset$. Then the Stein factorization W_f is also an almost-special polyhedron and we have a natural inclusion $S(P) \subset S(W_f)$. Apparently, each “region” of W_f is a planar surface. However, even if all the regions of P are planar surfaces, W_f is not homeomorphic to P in general.

- (3) In [20], the second-named author showed that the Heegaard genus of a closed orientable 3-manifold coincides with an invariant defined by branched spines. (See Endoh-Ishii [13] for details of the invariant.) Here, a spine of a closed 3-manifold M is an almost-special polyhedron P embedded in M so that M collapsed onto P after removing a small open ball from M . In other words, branched spines determine the minimal number of the critical points of Morse functions on M . Theorem 2.2 can be compared with this fact.

The following is a straightforward consequence of Theorem 2.2 (The case where M is closed and $L = \emptyset$ is proved by Kalmár-Stipsicz [18, Theorem 1.4]). See also (1) of the above remark.

Corollary 2.4. *Let M be a compact, orientable 3-manifold with (possibly empty) boundary consisting of tori and L a (possibly empty) link in M . Then there exists an S-map $f : (M, L) \rightarrow \mathbb{R}^2$ without cusp points satisfying $|\text{II}^2(f)| = \text{smc}(M, L)$ and $\text{II}^3(f) = \emptyset$.*

Lemma 2.5. *Let M_1 and M_2 be compact orientable 3-manifolds. Then $\text{bsc}(M_1 \# M_2) \leq \text{bsc}(M_1) + \text{bsc}(M_2)$.*

Proof. Let P_1 and P_2 be branched shadows of M_1 and M_2 , respectively. Choose an interior point p_i of a region of P_i for each $i \in \{1, 2\}$. By Costantino-Thurston [12, Lemma 3.2], the polyhedron P obtained by gluing small regular neighborhoods of p_1 and p_2 is a shadow of M (after putting the gleam 0 on the new disk region.) The polyhedron P apparently admits a branching. \square

By Theorem 2.2 and Lemma 2.5, the following holds.

Corollary 2.6. *Let M_1 and M_2 be compact orientable 3-manifolds with (possibly empty) boundary consisting of tori. Then we have $\text{smc}(M_1 \# M_2) \leq \text{smc}(M_1) + \text{smc}(M_2)$.*

Lemma 2.7. (1) *Let M_1 and M_2 be compact orientable 3-manifolds such that both of ∂M_1 and ∂M_2 contain torus components T_1 and T_2 , respectively. Let $\varphi : T_1 \rightarrow T_2$ be a diffeomorphism. Then $\text{bsc}(M_1 \cup_\varphi M_2) \leq \text{bsc}(M_1) + \text{bsc}(M_2)$.*

- (2) *Let M be a compact oriented 3-manifold such that ∂M contains at least two torus components T_1 and T_2 , which are equipped with the orientations induced from that of M . Let $\varphi : T_1 \rightarrow T_2$ be an orientation-reversing diffeomorphism. Then $\text{bsc}(M/\varphi) \leq \text{bsc}(M)$.*

Proof. (1) Let P_1 and P_2 be branched shadows of M_1 and M_2 , respectively. Let l_1 and l_2 be the boundary circles of P_1 and P_2 that correspond to the boundary tori T_1 and T_2 , respectively. By Costantino-Thurston [12, Proposition 3.27], a shadow P of $M_1 \cup_\varphi M_2$ is obtained by

$$P_1 \cup_{l_1=\alpha_1} Q \cup_{l_2=\alpha_2} P_2,$$

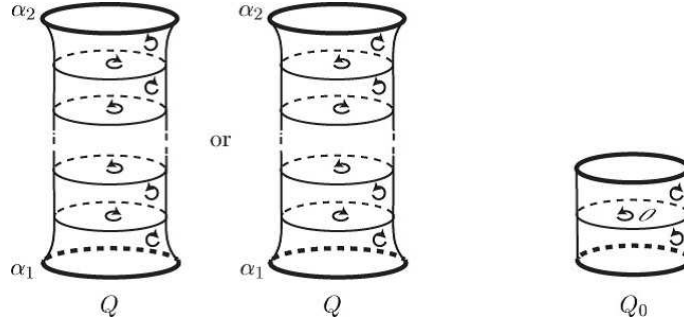


FIGURE 17. Branched shadows in the thickened torus.

where Q is one of the two oriented polyhedra shown in Figure 17 equipped with certain gleams. Then the orientations of the regions of Q shown in the figure extends to the whole of P , after reversing the orientations of the regions of P_1 or P_2 , if necessary.

(2) Let P_1 be a branched shadow of M . Let l_1 and l_2 be the boundary circles of P_1 that correspond to the boundary tori T_1 and T_2 , respectively. As in (1), the polyhedron P obtained by attaching Q along the loops l_1 and l_2 is a shadow of $\text{bsc}(M/\varphi)$. If the orientations of the regions of Q shown in the figure extends to the whole of P we are done. Otherwise, we first attach a shadow polyhedron Q_0 shown on the right-hand side in Figure 17, to Q along α_1 and then we apply the former operation using $Q_0 \cup Q$ instead of Q . This does not affect the topology of the resulting manifold, and now we may extend the orientation of the regions of $Q_0 \cup Q$ to the whole of P . \square

Theorem 2.2 and Lemma 2.7 yield the following:

- Corollary 2.8.** (1) *Let M_1 and M_2 be compact orientable 3-manifolds with boundary consisting of tori. Choose a component T_i of ∂M_i for each $i \in \{1, 2\}$. Let $\varphi : T_1 \rightarrow T_2$ be a diffeomorphism. Then $\text{smc}(M_1 \cup_\varphi M_2) \leq \text{smc}(M_1) + \text{smc}(M_2)$.*
- (2) *Let M be a compact oriented 3-manifold with boundary consisting of at least two tori. Choose two components T_1 and T_2 of ∂M , and equip them with the orientations induced from that of M . Let $\varphi : T_1 \rightarrow T_2$ be an orientation-reversing diffeomorphism. Then $\text{smc}(M/\varphi) \leq \text{smc}(M)$.*

For a link L in a 3-manifold M , we denote by $E(L)$ its exterior, that is, the complement of an open tubular neighborhood of L .

Lemma 2.9. *Let M be a compact orientable 3-manifold with (possibly empty) boundary consisting of tori, and let L be a link in M . Then we have $\text{bsc}(M) \leq \text{bsc}(M, L) = \text{bsc}(E(L))$.*

Proof. The left equality follows immediately from the definition.

We recall that a disk equipped with the gleam 0 is a branched shadow of $D^2 \times S^1$. Hence by Lemma 2.7 we have

$$\text{bsc}(M, L) \leq \text{bsc}(E(L)) + \text{bsc}(D^2 \times S^1) = \text{bsc}(E(L)).$$

The other inequality follows from the fact that by changing the colors of the boundary circles of a given branched shadow of (M, L) corresponding to L , which are all “ i ”, to “ e ”, we get a branched shadow of $E(L)$. \square

By Theorem 2.2 and Lemma 2.9 we have the following:

Corollary 2.10. *Let M be a compact, orientable 3-manifold with (possibly empty) boundary consisting of tori and L a link in M . Then we have $\text{smc}(M) \leq \text{smc}(M, L) = \text{smc}(E(L))$.*

We recall that a compact orientable 3-manifold is called a *graph manifold* if we can cut it off by embedded tori into S^1 -bundles over surfaces. A (possibly empty) link in a compact orientable 3-manifold is called a *graph link* if its exterior is a graph manifold.

Proposition 2.11. *Let M be a compact, orientable 3-manifold with (possibly empty) boundary consisting of tori and L a (possibly empty) link in M . Then the following conditions are equivalent:*

- (1) $\text{sc}(M, L) = 0$
- (2) $\text{bsc}(M, L) = 0$
- (3) L is a graph link.

Proof. By definition, (1) follows from (2). Also, by the proof of Costantino-Thurston [12, Proposition 3.31], (3) follows from (1). Below we show that (2) follows from (3). Suppose that L is a graph (possibly empty) link. By Lemma 2.9, it suffices to show that $\text{bsc}(E(L)) = 0$. By Saeki [36], there exists an S-map $f : E(L) \rightarrow S^2$ such that $f|_{S(f)}$ is a smooth embedding. In particular, f has no singular fibers of types II^2 or II^3 , and hence $\text{smc}(E(L)) = 0$. Thus by Corollary 2.10 we have $\text{smc}(M, L) = 0$. Now we get $\text{bsc}(M, L) = 0$ by Theorem 2.2. \square

3. STABLE MAPS OF LINKS

In this section we will always identify S^1 with $\mathbb{R}/2\pi\mathbb{Z}$.

Let D be a flat oriented disk properly embedded in the standard 4-ball B^4 , and let D' be the closure of $D \setminus \text{Nbd}(\partial D; D)$. Let $\pi : S^3 \rightarrow D$ be the projection induced by a collapsing $B^4 \searrow D$. We may assume without loss of generality that the preimage $V_h = \pi^{-1}(D')$ is a solid torus, that we identify with $D' \times S^1$, and $\pi|_{V_h}$ is an S-map without singular points. We put $V_v = S^3 \setminus \text{Int } V_h$. Let $L = L_1 \sqcup L_2 \sqcup \cdots \sqcup L_n$ be an n -component link in S^3 . We can push L by isotopy so that L lies in $D' \times [[-\varepsilon], [+ \varepsilon]]$, where ε is a sufficiently small positive real number, and $\pi|_{V_h}$ is generic with respect to L . The image $\pi(L)$, together with over/under crossing information at each double point, gives a diagram D_L for L on D' . Consider the mapping cylinder

$$P_{D_L}^* = ((L \times [0, 1]) \sqcup D') / (x, 0) \sim \pi(x).$$

Then $P_{D_L}^*$, together with a color “ i ” of each $L_j \times \{1\} \subset \partial P_L^* C$ is a shadow of (S^3, L) . Refer to Costantino-Thurston [12, Examples 3.15-17]. We fix an orientation of each component of L . The set of the regions of $P_{D_L}^*$ consists of subsurfaces of D' and $A_j = (L_j \times [0, 1]) / \sim$, $j \in \{1, 2, \dots, n\}$. To these subsurfaces of D' , we give the orientations induced by the prefixed orientation of D' . Also, we give an orientation to each A_j in such a way that

the induced orientation of $L_j \times \{1\}$ coincides with that of the prefixed orientation of L_j . See Figure 18. With these orientations of the regions, $P_{D_L}^*$ becomes a branched shadow

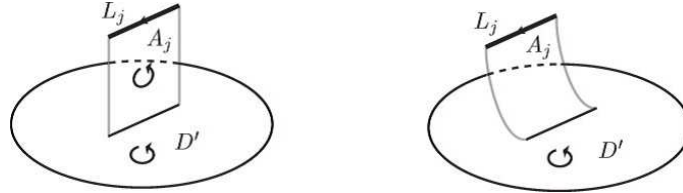


FIGURE 18. The branching on A_j .

of (S^3, L) . Let R be the region of $P_{D_L}^*$ touching $\partial D'$.

We say that the oriented link diagram D_L is *admissible* if R satisfies the following:

- the closure of R is diffeomorphic to an annulus; and
- on each component of $S(P_{D_L}^*) \setminus V(P_{D_L}^*)$ touched by R and A_j ($j \in \{1, 2, \dots, n\}$), these two regions induce the same orientation.

We note that if we choose, for example, D_L to be a closed braid presentation of L and give each component of L a suitable orientation, then R satisfies these conditions. If D_L is admissible, $P_{D_L} = P_{D_L}^* \setminus R$ is still a branched shadow of (S^3, L) . In the following we will discuss this branched shadow.

Let $f : (S^3, L) \rightarrow \mathbb{R}^2$ be a stable map constructed from P_L by the argument in Theorem 2.2. Let $S^3 \xrightarrow{q_f} W_f \xrightarrow{\bar{f}} S^2$ be the Stein factorization of f . From the construction of the stable map, we can identify the quotient space W_f with P_{D_L} in a natural way. The preimage of a point of P_{D_L} under the map q_f can be described as follows:

- (1) Let x_1 be a point in $D' \setminus P_{D_L}$. Then the preimage $q_f^{-1}(x_1)$, which is a regular fiber of f , is $\{x_1\} \times S^1 \subset V_h$. See Figure 19.

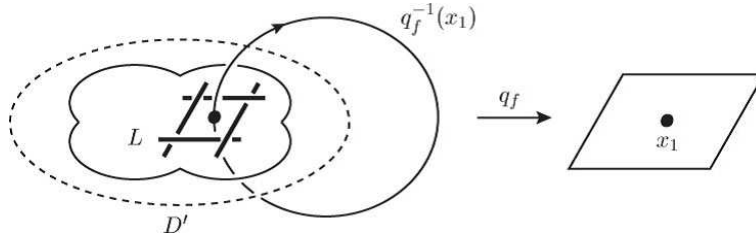
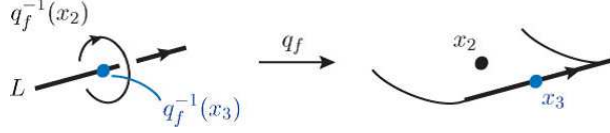
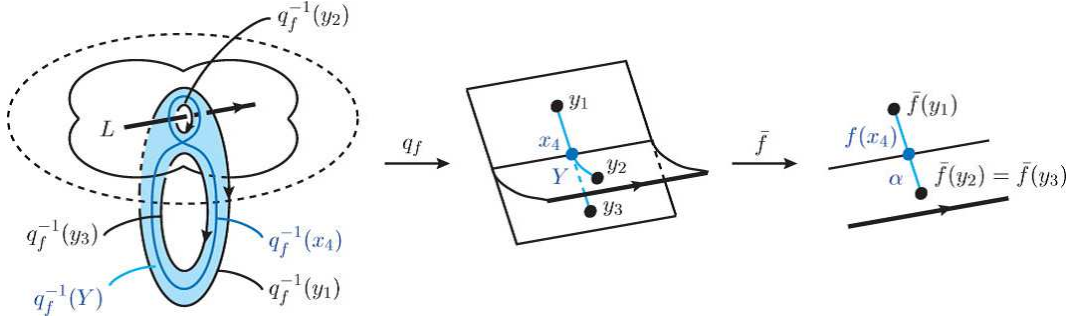


FIGURE 19. The configuration of a regular fiber.

- (2) Let x_2 be a point in $L_i \times (0, 1)$. Then the preimage $q_f^{-1}(x_2)$, which is also a regular fiber, is a meridian of L_i . See Figure 20.
- (3) Let x_3 be a point in $L_i \times \{1\}$. Then the preimage $q_f^{-1}(x_3)$, which is a singular fiber of type I^0 , is a point in L_i . See Figure 20.

FIGURE 20. The configuration of singular fiber of type I^0 .

- (4) Let x_4 be a point in $S(P_{D_L}) \setminus V(P_{D_L})$. Let α be a transverse arc for f at $\bar{f}(x_4)$. Then the preimage $Y = \bar{f}^{-1}(\alpha)$ is a Y-shaped graph. One endpoint of Y , say y_1 , is mapped to one endpoint of α by \bar{f} while the remaining two endpoints, say y_2 and y_3 , are mapped to the other endpoint of α . The preimage $q_f^{-1}(Y)$ is a pair of pants spanned by the three circles $q_f^{-1}(y_1)$, $q_f^{-1}(y_2)$ and $q_f^{-1}(y_3)$. Note that the configuration of these circles has already explained in Cases (1) and (2). Then the preimage $q_f^{-1}(x_4)$, which is a singular fiber of type I^1 , lies in $q_f^{-1}(Y)$ as a spine as illustrated in Figure 21.

FIGURE 21. The configuration of singular fiber of type I^1 .

- (5) Finally let x_5 be a true vertex of P_{D_L} . Let α be a transverse arc for f at $\bar{f}(x_5)$ as shown in Figure 22. Then the preimage $X = \bar{f}^{-1}(\alpha)$ is the X-shaped graph, i.e., the cone on four points. One endpoint of X , say y_1 , is mapped to one endpoint of α by \bar{f} while the remaining three endpoints, say y_2 , y_3 and y_4 , are mapped to the other endpoint of α . The preimage $q_f^{-1}(X)$ is a disk with three holes spanned by the four circles $q_f^{-1}(y_1)$, $q_f^{-1}(y_2)$, $q_f^{-1}(y_3)$ and $q_f^{-1}(y_4)$. Note, again, that the configuration of these circles has already explained in Cases (1) and (2). Then the preimage $q_f^{-1}(x_5)$, which is a singular fiber of type II^2 , lies in $q_f^{-1}(X)$ as a spine as illustrated in Figure 22.

Let L be a link in S^3 . Recall that the *crossing number* of L , denoted by $\text{cr}(L)$, is the minimal number of crossings in any of its diagrams on \mathbb{R}^2 .

Lemma 3.1. *Let L be an oriented non-split link in S^3 . There exists a diagram D_L for L on an oriented disk with $\text{cr}(L)$ crossing points such that D_L becomes admissible after reversing the orientations of all link components if necessary.*

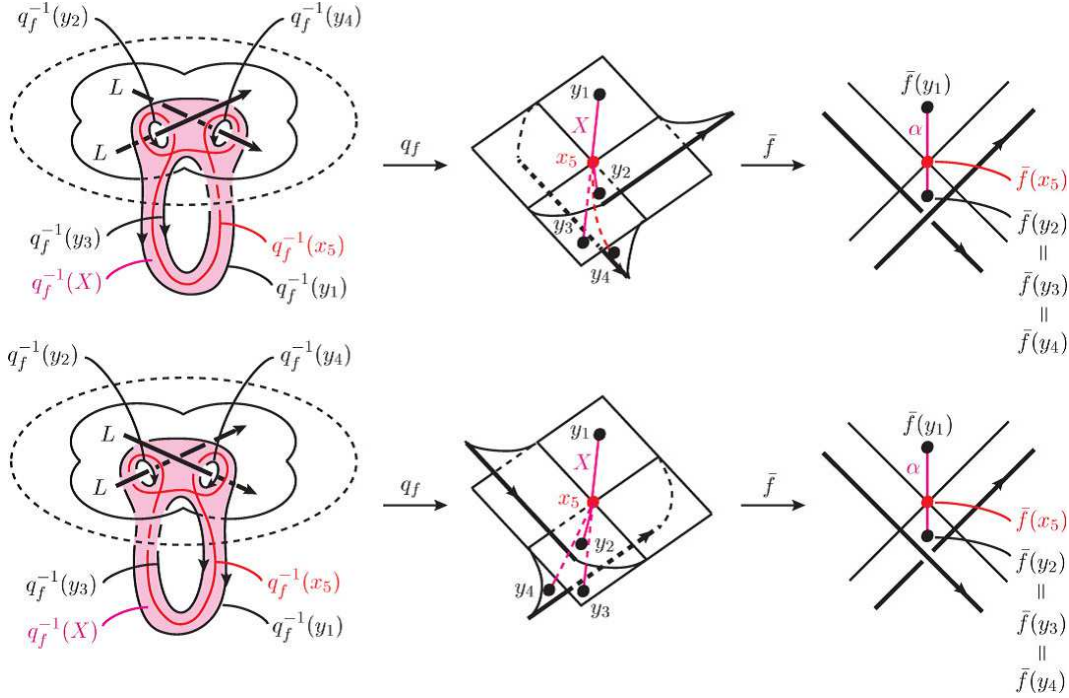


FIGURE 22. The configuration of singular fiber of type II^2 .

Proof. We start with a diagram D_L for L on the oriented 2-sphere S^2 with minimal crossing number. Using Seifert's algorithm for D_L we get a disjoint collection $\{c_1, c_2, \dots, c_m\}$ of circles on S^2 . We refer to, for instance, Rolfsen [35] for Seifert's algorithm. Let d be an open disk component of $S^2 \setminus \bigcup_{i=1}^m c_i$. Let D be a disk obtained by removing a small open neighborhood of an interior point of d . We equip D with the orientation induced by that of S^2 . Then the diagram D_L on D with the orientation of L or its inverse, is the required diagram for L . \square

The next theorem immediately follows from the above argument and Lemma 3.1.

Theorem 3.2. *For a link L in S^3 , there exists a proper stable map $f : (S^3, L) \rightarrow \mathbb{R}^2$ without cusp points such that*

- (1) *the Stein factorization W_f is contractible; and*
- (2) $|\text{II}^2(f)| \leq \text{cr}(L) - 2$ and $\text{II}^3(f) = \emptyset$.

Further, the configuration of both the regular and singular fibers of f can be described using a diagram of L .

Example 3. The left-hand side in Figure 23 shows an admissible diagram D_K of the figure-eight knot K . The right-hand side in the figure illustrates the contractible branched polyhedron P_{D_K} constructed from D_K . Then we have a proper stable map $f : (S^3, K) \rightarrow \mathbb{R}^2$ with Stein factorization $(S^3, K) \xrightarrow{q_f} P_{D_K} \xrightarrow{\bar{f}} \mathbb{R}^2$ such that $|\text{II}^2(f)| = 2$, $\text{II}^3(f) = \emptyset$

and $C(f) = \emptyset$. The configuration of the preimages of the points x_1, x_2, \dots, x_6 in P_{D_K} is shown in the figure.

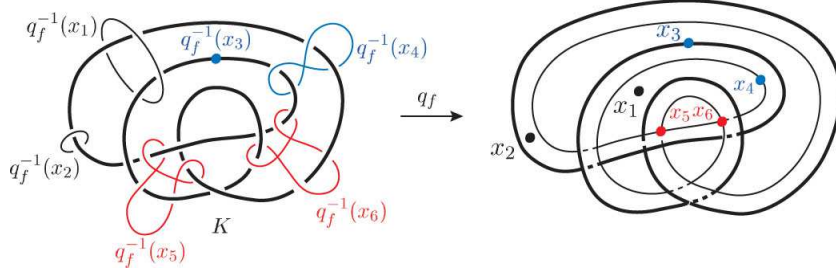


FIGURE 23. Regular and singular fibers of a stable map of the figure-eight knot. $q_f^{-1}(x_1)$ and $q_f^{-1}(x_2)$ are regular fibers of f . $q_f^{-1}(x_3)$ is a singular fiber of type I^0 . $q_f^{-1}(x_4)$ is a singular fiber of type I^1 . $q_f^{-1}(x_5)$ and $q_f^{-1}(x_6)$ are singular fibers of type II^2 .

From Corollary 2.10 and Theorem 3.2, the following holds:

Corollary 3.3. *Let M be a closed orientable 3-manifold obtained from S^3 by surgery along a link $L \subset S^3$. Then there exists a stable map $f : M \rightarrow \mathbb{R}^2$ without cusp points such that $|\text{II}^2(f)| \leq \text{cr}(L) - 2$ and $\text{II}^3(f) = \emptyset$.*

Remark 3.4. A result similar to Corollary 3.3 is obtained in Kalmár-Stipsicz [18, Theorem 1.2]. The numbers of singular fibers of types II^2 and II^3 , and cusp points in our Corollary 3.3 are less than theirs (in particular, $C(f) = \emptyset$ in our result).

4. KNOTS WITH BRANCHED SHADOW COMPLEXITY 1

In this section, we use the arguments in the previous section to characterize hyperbolic links in S^3 whose exteriors have stable map complexity 1. .

Lemma 4.1. *Let P be a shadow of a compact orientable 3-manifold M . Suppose that P is embedded in a compact orientable smooth 4-manifold W in a locally flat way so that $W \setminus P \cong \partial W \times (0, 1]$. Let $\pi : M \rightarrow P$ be a projection given by a collapsing $W \searrow P$. Then the homomorphism $\pi_1(M) \rightarrow \pi_1(P)$ induced by π is an epimorphism.*

Proof. The proof follows immediately from the fact that every closed curve l in P can be lifted to a closed curve \tilde{l} in M . \square

In the following, let U_1, U_2, U_3 and U_4 be the diagrams of the trivial knot illustrated in Figure 24.

Lemma 4.2. *Let M be a closed orientable 3-manifold that does not contain non-separating tori, and let P be a shadow of M . Then any simple closed curve in a region of P separates P .*

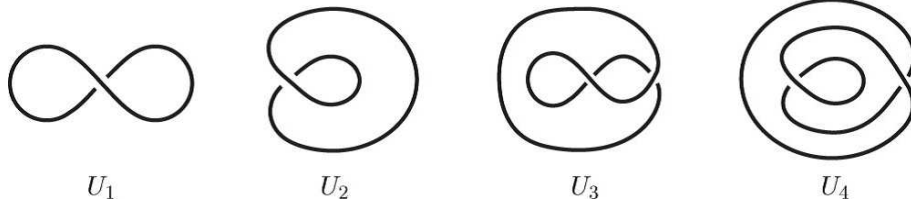


FIGURE 24. The diagrams U_1, U_2, \dots, U_4 of the trivial knot.

Proof. Let $\pi : M \rightarrow P$ be a projection as in Lemma 4.1. If a simple closed curve l in a region of P does not separate P , then $\pi^{-1}(l)$ is a non-separating torus in M , which is a contradiction. \square

Theorem 4.3. *Let K be a hyperbolic knot in S^3 . Then (S^3, K) admits a branched shadow P such that $c(P) = 1$ and $S(P)$ is connected if and only if K is one of the knots shown in Figure 25.*

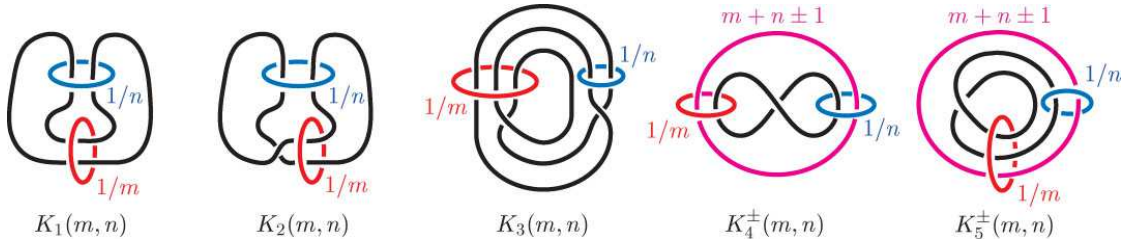


FIGURE 25. The knots admitting a branched shadow with one vertex and connected singular set.

Remark 4.4. Using *Conway's normal form*, the knots $K_1(m, n)$ and $K_2(m, n)$ can be written as $C(2n, 2m)$ and $C(2n, 2m + 1)$, respectively. Also, $K_4^\pm(m, n)$ is a knot obtained by performing Dehn surgery on one component of $C(2n + 1, 2m + 1)$ with the coefficients $m + n \pm 1$. The knot $K_3(m, n)$ is the *twisted torus knot* $T(3, 3m + 2; 2, n)$, see Callahan-Dean-Weeks [6] for the definition.

Proof. Suppose that (S^3, K) admits a branched shadow P such that $c(P) = 1$ (so $|V(P)| = 1$ and $|BV(P)| = 0$) and $S(P)$ is connected. Then $S(P)$ is one of the two graphs shown in Figure 26. Suppose that $S(P)$ is the one shown on the left-hand side

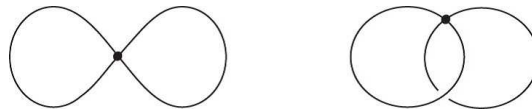
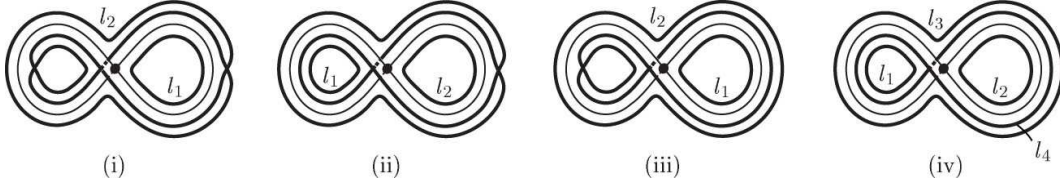


FIGURE 26. Two types of $S(P)$.

in the figure. Then its neighborhood $\text{Nbd}(S(P); P)$ in P is isomorphic to one of the

FIGURE 27. Four possible shapes of $\text{Nbd}(S(P); P)$.

four models illustrated in Figure 27. By Lemmas 4.1 and 4.2, each loop of the boundary of $\text{Nbd}(S(P); P)$ separates P , and P is a simply connected polyhedron obtained from $\text{Nbd}(S(P); P)$ by capping off some of the boundary components by disks. Case (i) is impossible because we can not obtain a simply connected polyhedron no matter how we cap off boundary components of $\text{Nbd}(S(P); P)$ by disks.

In Case (ii), P is simply connected if and only if P is obtained from $\text{Nbd}(S(P); P)$ by capping off the boundary components l_1 and l_2 by disks. We denote the two disk regions corresponding to l_1 and l_2 by D_1 and D_2 , respectively. Then as a branched polyhedron P is isomorphic to P_{U_3} , see the left-hand side in Figure 28. Note that in this case, the

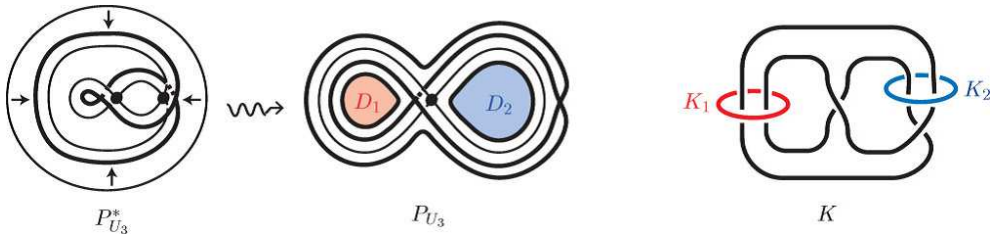


FIGURE 28. The link in Case (ii) in Figure 27.

regions D_1 and D_2 are equipped with the gleams $1/2$ and 1 , respectively. Moreover, we note that for each $i \in \{1, 2\}$, the preimage of an interior point of D_i under the projection $\pi : S^3 \rightarrow P$ is a trivial loop K_i illustrated on the right-hand side in Figure 28. In general, the gleams of the regions D_1 and D_2 are $1/2 + m$ and $1 + n$, respectively, where m, n are integers. Then the shadowed branched polyhedron P is a branched shadow of a knot K shown on the right-hand side in Figure 28, where we perform the Dehn surgeries on K_1 and K_2 with the coefficients $1/m$ and $1/n$, respectively. Hence K is the knot $K_2(m, n)$ shown in Figure 25.

In Case (iii) P is simply connected if and only if P is obtained from $\text{Nbd}(S(P); P)$ by capping off the boundary components l_1 and l_2 by disks. Then as a branched polyhedron P is isomorphic to P_{U_4} . In the same manner as in Case (ii), we can see that K is the knot $K_3(m, n)$ shown in Figure 25.

In Case (iv), P is simply connected if and only if P is obtained from $\text{Nbd}(S(P); P)$ in one of the following ways:

- (1) Cap off the boundary components l_i and l_j by disks, where $\{i, j\} = \{1, 2\}, \{1, 3\}, \{1, 4\}, \{2, 3\}$, or $\{2, 4\}$.
- (2) Cap off the boundary components l_i, l_j and l_k by disks, where $\{i, j, k\} = \{1, 2, 3\}, \{1, 2, 4\}, \{1, 3, 4\}$ or $\{2, 3, 4\}$.

In Case (1), P is isomorphic to $P_{U_1}^*$ or $P_{U_2}^*$ and hence it is easily seen that K is one of the knots shown in Figure 29. It follows that K is the trivial knot or the $(2, m+1)$ -torus

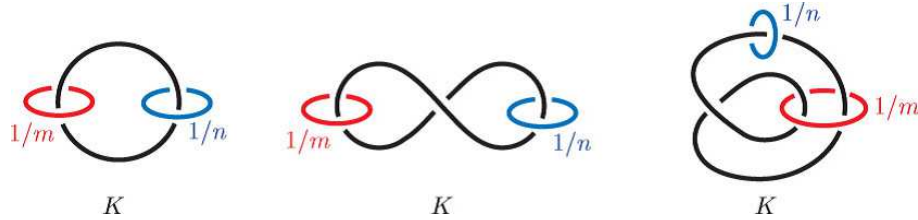


FIGURE 29. The links in Case(iv)-(1).

knot, where m is an integer. This contradicts the assumption that K is hyperbolic. Next we consider Case (2). If $\{i, j, k\} = \{1, 2, 3\}$, then P is obtained by capping off the boundary component of $P_{U_1}^*$ that does not correspond to the trivial knot U_1 by a disk. We denote the two disk regions of $P_{U_1}^*$ by D_1 and D_2 . We note that the both gleams on D_1 and D_2 defined by the construction of $P_{U_1}^*$ are $+1/2$. The two boundary circles K and K' of $P_{U_1}^*$ together with the preimages K_1 and K_2 of interior points of D_1 and D_2 , respectively, under the projection $\pi : S^3 \rightarrow P$ form the minimally twisted 4-chain link. The changing of the gleams on D_1 and D_2 to $1/2 + m$ and $1/2 + n$, respectively, where m, n are integers, corresponds to Dehn surgeries on K_1 and K_2 with the coefficients $1/m$ and $1/n$, respectively. Moreover, the capping off of $K' \subset \partial P_{U_1}^*$ by a disk corresponds to a Dehn surgery on K' with the coefficients p , where p is an integer, see Figure 30. Hence

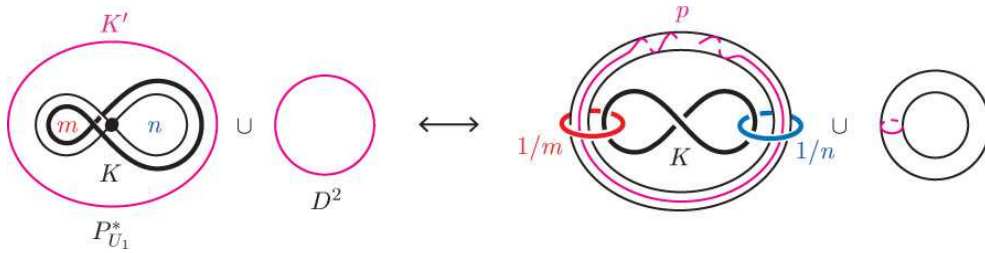


FIGURE 30. The link in the case $\{i, j, k\} = \{1, 2, 3\}$ or $\{1, 2, 4\}$.

P is a branched shadow of a knot in $L(p - m - n, 1)$, thus $p = m + n \pm 1$ by assumption. In this case, K is the knot $K_4^\pm(m, n)$ shown in Figure 25. The same arguments apply to the case $\{i, j, k\} = \{1, 2, 4\}$. If $\{i, j, k\} = \{1, 3, 4\}$ or $\{2, 3, 4\}$, then P is obtained by capping off the boundary component of $P_{U_2}^*$ that does not correspond to the trivial knot U_2 by a disk. By a similar argument as above, K is a knot described in Figure 31, where

m, n, p are integers. Again, P is a branched shadow of a knot in $L(p - m - n, 1)$, thus

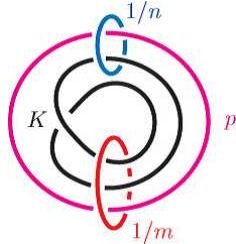


FIGURE 31. The link in the case $\{i, j, k\} = \{1, 3, 4\}$ or $\{2, 3, 4\}$.

$p = m + n \pm 1$ by assumption. In this case, K is the knot $K_5^\pm(m, n)$ shown in Figure 25.

Next, suppose that $S(P)$ is the one shown on the right-hand side in Figure 26. Then its neighborhood $\text{Nbd}(S(P); P)$ in P is homeomorphic to one of the four models illustrated in Figure 32. None of Cases (i)-(iii) is possible because we can not obtain a simply

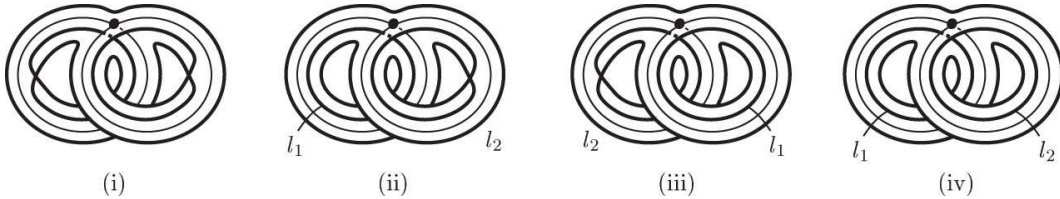


FIGURE 32. The other four shapes of $\text{Nbd}(S(P); P)$.

connected polyhedron no matter how we cap off boundary components of $\text{Nbd}(S(P); P)$ by disks.

In Case (iv), P is simply connected if and only if P is obtained from $\text{Nbd}(S(P); P)$ by capping off the boundary components l_1 and l_2 by disks. We denote the two disk regions corresponding to l_1 and l_2 by D_1 and D_2 , respectively. We may embed P into S^3 in such a way that P is a spine of S^3 , that is, S^3 collapses onto P after removing a small open 3-ball. Then the 3-thickening of P can be realized as a regular neighborhood $\text{Nbd}(P; S^3)$, which is homeomorphic to a closed 3-ball. We first consider the case where the both gleams of D_1 and D_2 are 0. As observed in Costantino-Thurston [12, Lemma 3.24], the 4-manifold reconstructed from P is $\text{Nbd}(P; S^3) \times [-1, 1] \cong B^4$ and hence P is a branched shadow of S^3 . Moreover, the boundary of B^4 , which is S^3 , can be identified with the union of $\text{Nbd}(P; S^3)$ and its mirror image glued along their boundaries by the canonical identity. The collapsing $B^4 \rightarrow P$ is obtained by combining two collapsings $\text{Nbd}(P; S^3) \searrow P$ and $[0, 1] \searrow \{0\}$. Let k_1 and k_2 be the preimages of interior points of D_1 and D_2 , respectively, under the collapsing $\text{Nbd}(P; S^3) \searrow P$. Then on the boundary of B^4 , the two copies of each k_i give rise to a simple closed curve K_i as described in Figure 33. In particular, we see that $K \sqcup K_1 \sqcup K_2$ is the Borromean link. In the case where the gleams of D_1 and D_2 are m and n , respectively, where m, n are integers, K is

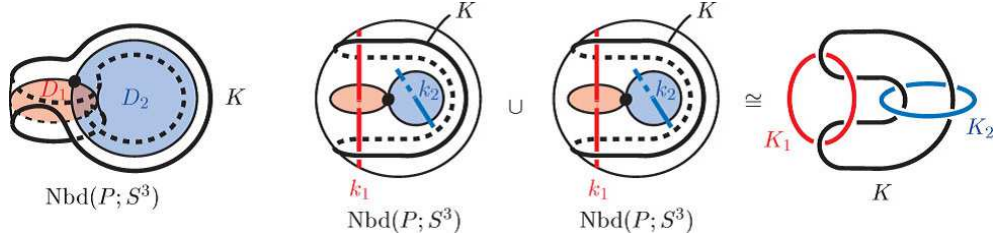


FIGURE 33. The link in Case (iv) in Figure 32.

the knot in S^3 obtained by the Dehn surgeries on K_1 and K_2 with the coefficients $1/m$ and $1/n$, respectively. Hence K is the knot $K_1(m, n)$ shown in Figure 25.

Conversely, suppose that $K \subset S^3$ is a hyperbolic knot shown in Figure 25. By the above arguments, (S^3, K) admits a branched shadow P such that $c(P) = 1$ and $S(P)$ is connected. This completes the proof. \square

We call the almost-special polyhedron of the shape depicted in Figure 34 a *tower*. We

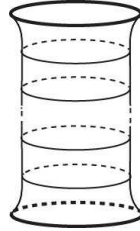


FIGURE 34. A tower.

require that a tower contains at least one disk region.

Lemma 4.5. *Let L be a hyperbolic link in S^3 with $\text{bsc}(S^3, L) = 1$, and let P be a branched shadow of (S^3, L) with $c(P) = 1$. Let P' be a regular neighborhood of the component of $S(P)$ containing the vertex. Then there exists a branched shadow P'' of (S^3, L) which is obtained from P' by attaching towers to some of its boundary components.*

Proof. Let l be a component of $\partial P'$. By Lemma 4.2, l separates P into two components P_1 and P_2 . Without loss of generality we can assume that P_1 is the component containing the vertex. It suffices to show that we can replace P_2 with a tower Q so that the resulting shadowed polyhedron $P_1 \cup_l Q$ is again a branched shadow of (S^3, L) . Let $\pi : S^3 \rightarrow P$ be a projection as in Lemma 4.1. We set $M_i = \pi^{-1}(P_i)$ ($i = 1, 2$) and $T = \pi^{-1}(l)$. Then at least one of M_1 and M_2 is a solid torus.

Suppose that T is parallel to $\partial \text{Nbd}(K)$ in $E(L)$, where K is a component of L . If K is in M_1 then $M_1 \cap L = K$, and hence P_2 is a branched shadow of $E(L)$. Since P_2 has no vertices, it follows from Lemma 2.9 and Proposition 2.11 that $E(L)$ is a graph manifold, which contradicts the hyperbolicity of L . If K is in M_2 then $M_2 \cap L = K$, hence by replacing P_2 with a tower, we have a branched shadow of (S^3, L) .

Now we assume that T is not parallel to any component of $\partial\text{Nbd}(L)$. Suppose that M_i is a solid torus, where i is either 1 or 2.

First we consider the case where the solid torus M_i is knotted in S^3 , that is, M_{3-i} is not a solid torus. If $M_i \cap L$ is empty, we can attach a tower Q to P_{3-i} along l so that the resulting polyhedron $P_{3-i} \cup_l Q$ is again a branched shadow of (S^3, L) after giving suitable gleams to its regions. If $i = 1$, then $\text{bsc}(S^3, L) = 0$, which contradicts the hyperbolicity of L . Hence we have $i = 2$, which is our assertion. Suppose that $M_i \cap L$ is not empty. If $M_i \cap L$ is not contained in a 3-ball in M_i , then T is an essential torus in $E(L)$. By Thurston's Hyperbolization Theorem [40, 28, 29, 30, 19] this implies L is not hyperbolic, which is a contradiction. If $M_i \cap L$ is contained in a 3-ball in M_i , then either L is a split link or $M_{3-i} \cap L = \emptyset$. The former case contradicts the hyperbolicity of L . In the latter case, we can attach a tower Q to P_i along l so that the resulting polyhedron $P_i \cup_l Q$ is again a branched shadow of (S^3, L) after giving suitable gleams to its regions. Note that the operation replacing P_{3-i} by Q corresponds to a Fox re-embedding of M_i , and under this re-embedding the knot type of L does not change since L is contained in a 3-ball in M_i . If $i = 2$, then $\text{bsc}(L) = 0$, which contradicts the hyperbolicity of L . Hence we have $i = 1$, which is our assertion.

Next we consider the case where M_i is unknotted, that is, M_{3-i} is also a solid torus. Since L is hyperbolic and T is not parallel to any component of $\partial\text{Nbd}(L)$, we have either $L \subset M_1$ or $L \subset M_2$, otherwise T is an essential torus in $E(L)$ or L is a split link. If $L \subset M_2$ then, attaching a tower to P_2 , we obtain a branched shadow without vertices. Hence we have $L \subset M_1$. Then attaching a tower to P_1 , we obtain a branched shadow of (S^3, L) , which is our assertion. \square

Theorem 4.6. *Let L be a hyperbolic link in S^3 . Then $\text{bsc}(S^3, L) = 1$ if and only if the exterior of L is diffeomorphic to a 3-manifold obtained by Dehn filling the exterior of one of the six links L_1, L_2, \dots, L_6 in S^3 along some of (possibly none of) boundary tori of its exterior, where L_1, L_2, \dots, L_6 are illustrated in Figure 2.*

Proof. Let P be a branched shadow of (S^3, L) with one vertex. By Lemma 4.1, P is simply connected. Let P' be a regular neighborhood of the component of $S(P)$ containing the vertex. Then P' is isomorphic to one of the eight models illustrated in Figures 27 and 32. By Lemma 4.5, we may assume that P is obtained from P' by attaching towers to some of its boundary components. It follows from Seifert-van Kampen Theorem that P can be simply connected if and only if P' is isomorphic to one of the eight models except Figure 32 (i). Thus it suffices to find a hyperbolic link L in S^3 for each of the remaining seven models such that the shadow P' equipped with “ e ” on each of the components of $\partial P'$ is a branched shadow of the exterior $E(L)$. By Theorem 4.3, these links for Figure 27 (ii), (iii), (iv) and Figure 32 (iv) are already obtained as follows: (Note that the links L_3, L_4, L_6 are those used to define the knots $K_1(m, n), K_2(m, n), K_4^\pm(m, n)$, respectively, though each of them is depicted in a different way.)

- (1) If P' is isomorphic to the model shown in Figure 27 (ii), then P' is a branched shadow of the exterior of L_4 .
- (2) If P' is isomorphic to the model shown in Figure 27 (iii), then P' is a branched shadow of the exterior of L_5 .

- (3) If P' is isomorphic to the model shown in Figure 27 (iv), then P' is a branched shadow of the exterior of L_6 .
- (4) If P' is isomorphic to the model shown in Figure 32 (iv), then P' is a branched shadow of the exterior of L_3 .

Suppose that P' is isomorphic to the model shown in Figure 27 (i). Then P is obtained from P' by attaching towers to each of the boundary components l_1, l_2 of P' , otherwise P will not be simply-connected. Note that, in this case, $S(P)$ is not connected. Let P_0 be an almost-special polyhedron obtained by capping off l_1 and l_2 by disks, where l_1 and l_2 are the boundary components of $\text{Nbd}(S(P); P)$ as shown in Figure 27 (i). Then as a polyhedron P_0 is a spine of S^3 that is called the *abalone* shown in Figure 35. See, for instance, Ikeda [16] and Matveev [27] for details of this spine. We denote the

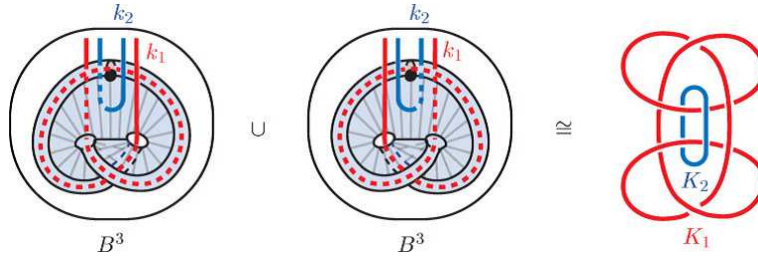


FIGURE 35. The link in Case (i) in Figure 27.

two disk regions corresponding to l_1 and l_2 by D_1 and D_2 , respectively. If we assume that both gleams of D_1 and D_2 are 0, then the 3-thickening of P_0 can be realized as a regular neighborhood $\text{Nbd}(P_0; S^3)$, which is homeomorphic to a closed 3-ball. Then as in the case of Figure 32 (iv) of Theorem 4.3, the 4-manifold reconstructed from P_0 is $\text{Nbd}(P_0; S^3) \times [-1, 1] \cong B^4$ and hence P_0 is a branched shadow of S^3 . Moreover, the boundary of B^4 can be identified with the union of $\text{Nbd}(P_0; S^3)$ and its mirror image glued along their boundaries by the canonical identity. The collapsing $B^4 \searrow P$ is obtained by combining two collapsings $\text{Nbd}(P_0; S^3) \searrow P_0$ and $[0, 1] \searrow \{0\}$. Let k_1 and k_2 be the preimages of interior points of D_1 and D_2 , respectively, under the collapsing $\text{Nbd}(P_0; S^3) \searrow P_0$. Then on the boundary of B^4 , the two copies of each k_i give rise to a simple closed curve K_i as described in Figure 35. Then the link $K_1 \cup K_2 \subset S^3$ is L_1 . This implies that P' equipped with the color “e” on each of the component of $\partial P'$ is a branched shadow of the exterior $E(L_1)$.

We remark that Figure 32 (ii) and (iii) are isomorphic by the reflection. Suppose that P' is isomorphic to the model shown in Figure 32 (ii). Then P is obtained from P' by attaching a tower to each of the boundary components l_1, l_2 of P' , otherwise P will not be simply-connected. Again in this case, $S(P)$ is not connected. Let v be the vertex of P' . Let $\text{Nbd}(v; P) \subset P'$ be a regular neighborhood such that $P' \setminus \text{Nbd}(v; P)$ consists of two components P_1 and P_2 , where each of P_1 and P_2 is isomorphic to the direct product of a Y-shaped graph and an interval. We assume that $P_1 \cap l_1 \neq \emptyset$ (so $P_2 \cap l_1 = \emptyset$). Then $\text{Nbd}(v; P) \cup P_1$ is a shadow of the 3-manifold M_1 shown in Figure 36 while P_2 is a shadow of the direct product M_2 of a pair of pants and an interval shown in the same

figure. We may glue M_1 and M_2 along the pair of pants as indicated in the figure to

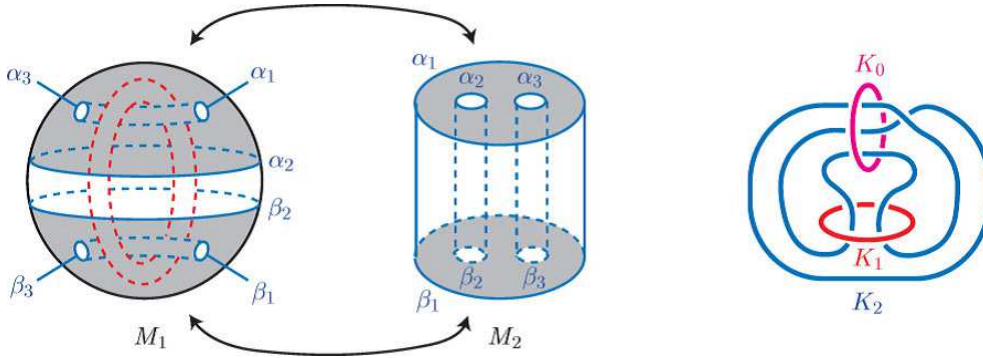


FIGURE 36. The link in Cases (ii) and (iii) in Figure 32.

get a 3-manifold M presented by the branched shadow P' . Let $K_0 \cup K_1 \cup K_2$ be the link shown on the right-hand side in Figure 36. It is easy to see that M is the exterior of $K_1 \cup K_2$ after performing Dehn surgery along K_0 with the coefficient 0. We want to describe M as the exterior of a link in S^3 . To do so, we perform Dehn surgery along K_2 with the coefficient 1. Let K_2^* be the core of the solid torus corresponding to K_2 in the surgered manifold. Since $K_0 \cup K_2$ is the Hopf link, the surgered manifold is S^3 and $K_1 \cup K_2^*$ is a link whose exterior is M . By an elementary argument of Dehn surgery, we may check that the link $K_1 \cup K_2^*$ is L_2 .

Conversely, suppose that $L \subset S^3$ is a hyperbolic link whose exterior is diffeomorphic to a 3-manifold obtained by Dehn filling the exterior of one of the six links L_1, L_2, \dots, L_6 in S^3 along some of (possibly none of) boundary tori of its exterior. By Proposition 2.11, $\text{bsc}(S^3, L) \geq 1$. Moreover, by the above arguments, (S^3, L) admits a branched shadow P with $c(P) = 1$. This completes the proof. \square

Remark 4.7. In Case (3) of the above proof, we can also use the 4-component link depicted in Figure 31 instead of L_6 . Actually, this link and L_6 have the diffeomorphic complements.

From Theorems 2.2 and 4.6, the following holds:

Corollary 4.8. *Let L be a hyperbolic link in S^3 . Then there exists a stable map $f : (S^3, L) \rightarrow \mathbb{R}^2$ without cusp points such that $|\text{II}^2(f)| = 1$ and $\text{II}^3(f) = \emptyset$ if and only if the exterior of L is diffeomorphic to a 3-manifold obtained by Dehn filling the exterior of one of the six links L_1, L_2, \dots, L_6 in Theorem 4.6 along some of (possibly none of) boundary tori of its exterior.*

Since the correspondence between S-maps and branched shadows are so explicit, we can completely determine the configuration of the singular fibers of the S-maps from the branched shadows. In the rest of this section, we show the configuration of singular fibers of type II^2 for the links L_3, L_4, L_5 and L_6 in Theorem 4.6. We omit the other links L_1 and L_2 since the configuration seems to be more complicated.

Corollary 4.9. *For $i \in \{3, 4, 5, 6\}$, the exterior of the link L_i admits an S-map $f : E(L_i) \rightarrow \mathbb{R}^2$ with $c(f) = 1$ such that the configuration of the unique singular fiber of type Π^2 is shown in Figure 37.*

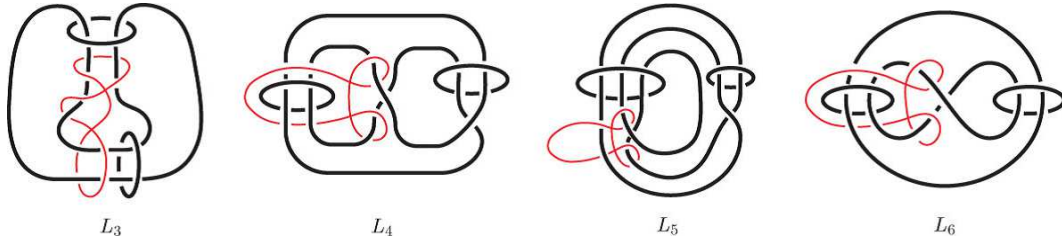


FIGURE 37. The configuration of singular fibers in Corollary 4.9.

Proof. Since the links L_4, L_5, L_6 admit branched shadows $P_{U_3}, P_{U_4}, P_{U_1}^*$, respectively, we get an S-map $f : E(L_i) \rightarrow \mathbb{R}^2$ ($i \in \{4, 5, 6\}$) with $c(f) = 1$ using these branched shadows and then we can find easily the configuration of its unique singular fiber of type Π^2 as shown in Figure 37, following the method introduced in Section 3. Hence it remains to show the case of L_3 . We recall that the exterior of L_3 admits a branched shadow P' depicted in Figure 32 (iv). We use the same notation as in the proof of Theorem 4.6, that is, l_1 and l_2 are the components of $\partial P'$ shown in Figure 32 (iv) and L_3 consists of 3 components K, K_1, K_2 as shown in Figure 33. Let $f : E(L_3) \rightarrow \mathbb{R}^2$ be an S-map with $c(f) = 1$ constructed from the branched shadow depicted in Figure 32 (iv) using the argument in Theorem 2.2. Then P' can be naturally identified with W_f , where $E(L_3) \xrightarrow{q_f} W_f \xrightarrow{\bar{f}} \mathbb{R}^2$ is the Stein factorization of f . We denote the vertex of P' by v . Let $x_1, x_2, \dots, x_6, y_1, y_2, \dots, y_6$ be the points on $\partial \text{Nbd}(v; P') \cap \partial P'$ shown on the left-hand side in Figure 38, and set $\partial \text{Nbd}(v; P') \cap S(P') = \{z_1, z_2, z_3, z_4\}$ as shown in the same figure. Let Y_i ($i \in \{1, 2, 3, 4\}$) be the closure of the Y-shaped component of $\partial \text{Nbd}(v; P') \setminus \partial P'$ containing z_i . Then by the argument in Theorem 4.3, $q_f^{-1}(x_3)$ and $q_f^{-1}(y_3)$ are longitudes of the trivial knot K_1 , and $q_f^{-1}(x_5)$ and $q_f^{-1}(y_5)$ are longitudes of K_2 , while all the other x_i 's and y_i 's are meridians of K . The preimage Y_i ($i \in \{1, 2, 3, 4\}$) is a pair of pants spanned by the simple closed curves $q_f^{-1}(\partial Y_i)$ as shown on the right-hand side in Figure 38. We note that once we fix an orientation of $E(L_3)$ and \mathbb{R}^2 , we may give an orientation of each of $q_f^{-1}(x_i)$ and $q_f^{-1}(y_i)$ ($i \in \{1, 2, \dots, 6\}$) in a natural way. Then by the branching of the Stein factorization P' , the preimage $q_f^{-1}(z_i)$, which is an immersed figure-8 shaped curve, lies in $q_f^{-1}(Y_i)$ as shown in the same figure. The union $\bigcup_{i=1}^4 q_f^{-1}(Y_i)$ cuts $E(L_3)$ into a genus 3 handlebody N_0 and two genus 2 handlebodies N_1, N_2 , where N_1 is bounded by $q_f^{-1}(Y_1)$ and $q_f^{-1}(Y_2)$, and N_2 is bounded by $q_f^{-1}(Y_3)$ and $q_f^{-1}(Y_4)$. We note here that each of N_1 and N_2 is the product (a pair of pants) $\times [0, 1]$ corresponding to the preimage of one of the two components of the closure of $P' \setminus \text{Nbd}(v; P')$ under q_f .

Now, the preimage $q_f^{-1}(v)$, which is our target, lies in H_0 . As reviewed in Section 1.2, $q_f^{-1}(\text{Nbd}(v; P'))$ has a standard product structure (a disk with 3 holes) $\times [0, 1]$ for which

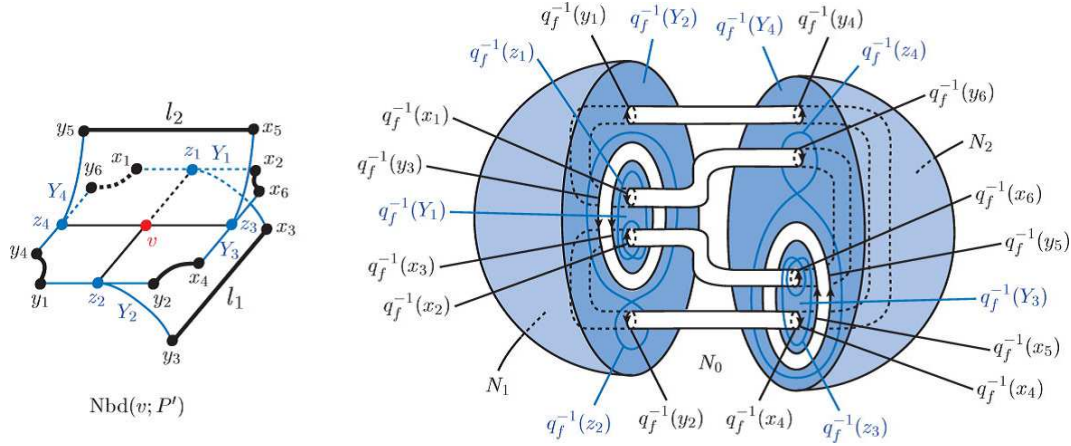


FIGURE 38. The configuration of singular fibers for L_3 .

the preimages of z_1, z_2, z_3, z_4 and v are illustrated on the left-hand side in Figure 39 (cf. Figure 8). The right-hand side in Figure 38 also gives a $(\text{a disk with 3 holes}) \times [0, 1]$ of

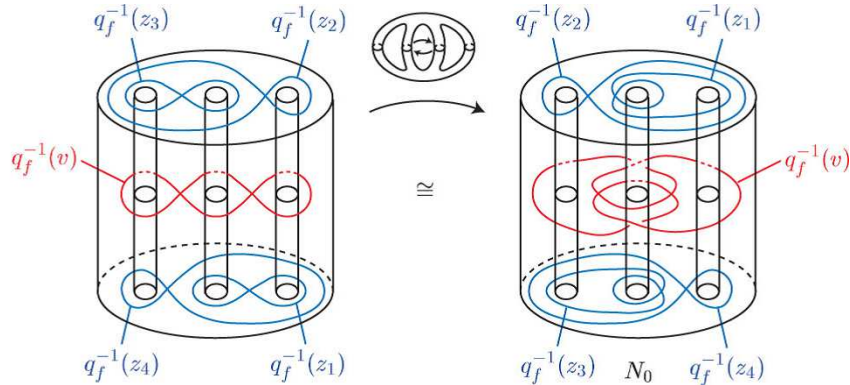


FIGURE 39. Twisting the handlebody.

the handlebody H_0 as shown on the right-hand side in Figure 39. However, this product structure is not consistent with the standard one. There exists an orientation-preserving diffeomorphism between the handlebodies, which is realized by switching the two handles as described in the figure. Using this diffeomorphism, we can find the configuration of $q_f^{-1}(v)$ inside N_0 . This completes the proof. \square

Example 4. The knot $K_2(1, 1)$ is the figure-eight knot. By Corollary 4.9 the exterior of $K_2(1, 1)$ admits an S-map with $c(f) = 1$ whose unique singular fiber of type II^2 is shown in Figure 40.

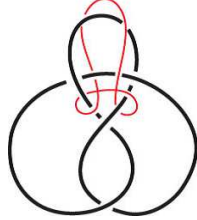


FIGURE 40. The configuration of the singular fiber of type II^2 in the figure-eight knot complement.

5. STABLE MAPS AND HYPERBOLIC VOLUME

Throughout the section, we consider a particular type of polyhedron, a *special polyhedron*. An almost-special polyhedron P is said to be *special* if there is no loop without vertices in $S(P)$ and each region of P is a disk. We note that in this case, $S(P)$ is connected and P contains no boundary vertices. We call a shadow of a 3-manifold that is a special polyhedron a *special shadow* of M . Remark that every closed orientable 3-manifold admits a branched, special shadow by the moves described in Turaev [42] and Costantino [7]. See also Martelli [25] for interesting properties of special shadows.

Let M be a closed orientable 3-manifold with special shadow P and $\pi : M \rightarrow P$ be the projection induced by the collapsing $W \searrow P$, where $M = \partial W$. Set $M_{S(P)} = \pi^{-1}(\text{Nbd}(S(P); P))$. Costantino-Thurston [12] showed that $M_{S(P)}$ admits a complete, finite volume hyperbolic structure realized by gluing $2c(P)$ copies of a regular ideal octahedron. Thus, in particular, we have $\text{vol}(M_{S(P)}) = 2c(P)V_{\text{Oct}}$. Since each region of a special polyhedron is a disk, M is obtained from $M_{S(P)}$ by attaching solid tori, i.e., by Dehn fillings. In particular, by the 6-Theorem of Agol [2] and Lackenby [22] and the Geometrization Theorem of Perelman [31, 32, 33], if all slope lengths of the Dehn fillings are more than 6 then M admits a complete finite volume hyperbolic structure. Since the hyperbolic structure of $M_{S(P)}$ is explicitly given by the ideal octahedra, the slope lengths of Dehn fillings can be calculated in terms of the combinatorial structure of the special polyhedron P and the gleams on its regions.

Let P be a shadowed, special polyhedron. For each region R of P , set $\text{sl}(R) = \sqrt{(2g)^2 + k^2}$, where $g \in \frac{1}{2}\mathbb{Z}$ is the gleam on R and k is an integer counting how many times the boundary of the closure of R passes through the vertices of P . We will show later, in Lemma 5.3, that $\text{sl}(R)$ is nothing but the slope length of the Dehn filling for the corresponding boundary torus when we obtain M from the hyperbolic manifold $M_{S(P)}$. We set $\text{sl}(P) = \min_R \text{sl}(R)$, where R varies over all regions of P .

Proposition 5.1. *Let M be a closed orientable 3-manifold. Let P be a branched, special shadow of M . If $\text{sl}(P) > 2\pi$, then we have*

$$\begin{aligned} 2 \text{smc}(M)V_{\text{Oct}} \left(1 - \left(\frac{2\pi}{\text{sl}(P)} \right)^2 \right)^{3/2} &\leq 2 c(P)V_{\text{Oct}} \left(1 - \left(\frac{2\pi}{\text{sl}(P)} \right)^2 \right)^{3/2} \\ &\leq \text{vol}(M) < 2 \text{smc}(M)V_{\text{Oct}}. \end{aligned}$$

Proof. The first inequality is immediate from the definition. The second inequality follows from Theorem 2.2, Lemma 5.3 below, and Futer-Kalfagianni-Purcell [14, Theorem 1.1]. The last inequality follows from Costantino-Thurston [12, Theorem 3.37] and Theorem 2.2. \square

From these inequalities we have the following result that concerns the coincidence of shadow complexities, branched shadow complexities and stable map complexities.

Theorem 5.2. *Let M be a closed orientable 3-manifold, and let P be a branched, special shadow of M . If $\text{sl}(P) > 2\pi\sqrt{2c(P)}$, then we have $\text{sc}(M) = \text{bsc}(M) = \text{smc}(M) = c(P)$.*

Proof. The inequality $\text{sl}(P) > 2\pi\sqrt{2c(P)}$ implies that

$$1 - \frac{1}{c(P)} < 1 - 2 \left(\frac{2\pi}{\text{sl}(P)} \right)^2 < \left(1 - \left(\frac{2\pi}{\text{sl}(P)} \right)^2 \right)^{3/2}.$$

Thus we have the following inequalities:

$$0 < c(P) - \text{sc}(M) \left(1 - \left(\frac{2\pi}{\text{sl}(P)} \right)^2 \right)^{3/2} < 1.$$

Since $\text{sc}(M)$, $\text{bsc}(M)$ and $\text{smc}(M)$ are all less than or equal to $c(P)$, the above inequalities hold even if we replace $c(P)$ by $\text{sc}(M)$, $\text{bsc}(M)$ and $\text{smc}(M)$. Applying this to the inequalities in Proposition 5.1, we have

$$0 \leq \text{smc}(M) - \frac{\text{vol}(M)}{2V_{\text{Oct}}} < 1.$$

By the way, it is easy to check that the inequalities in Proposition 5.1 hold not only for the stable map complexity but also the shadow complexity, the branched shadow complexity and the number of vertices of the polyhedron P . Therefore the above inequality holds even if we replace $\text{smc}(M)$ by $\text{sc}(M)$, $\text{bsc}(M)$ and $c(P)$. Since $\text{sc}(M)$, $\text{bsc}(M)$, $\text{smc}(M)$ and $c(P)$ are integers, they coincide. \square

Let P be a special shadow of a closed orientable 3-manifold M . Costantino-Thurston [12, Proposition 3.34] described the Euclidean structure on the cusps of $M_{S(P)}$ in terms of \mathbb{Z}_2 -gleam and the numbers of the vertices through which the boundaries of the regions of P runs. The proof of the following lemma is not essentially new. In fact, it is described implicitly in [12]. The maximal horocusp had been observed in Costantino-Frigerio-Martelli-Petronio [11] though gleams are excluded from the discussion. Therefore we believe that it deserves to be clarified in our setting with details.

Lemma 5.3. *Let P be a special shadow of a closed orientable 3-manifold M . Let R_1, R_2, \dots, R_n be the regions of P . Set $l_i = R_i \cap \partial\text{Nbd}(S(P); P)$, and let T_i be the component of the boundary of $M_{S(P)}$ corresponding to l_i for $i \in \{1, 2, \dots, n\}$. Then there exists a maximal horoball neighborhood $C = C_1 \cup C_2 \cup \dots \cup C_n$ of the cusps of the interior of $M_{S(P)}$, where C_i corresponds to T_i , such that M is obtained from $M_{S(P)}$ by Dehn fillings along the slopes $s_1 \subset T_1, s_2 \subset T_2, \dots, s_n \subset T_n$ whose lengths with respect to C are $\text{sl}(R_1), \text{sl}(R_2), \dots, \text{sl}(R_n)$, respectively.*

Proof. For each vertex v_i ($i \in \{1, 2, \dots, c(P)\}$), we set $P_i = \text{Nbd}(v_i; P)$. We regard $\text{Nbd}(S(P); P)$ as the union $\bigcup_{i=1}^{c(P)} P_i$. For the 3-dimensional thickening X_i of P_i , we fix a collapsing $\rho_i : X_i \searrow P_i$ so that:

- for a point y in $P_i \setminus S(P_i)$, $\rho_i^{-1}(y) = \{y\} \times [-1, 1]$;
- for a point y in $S(P_i) \setminus \{v_i\}$, $\rho_i^{-1}(y)$ is a Y-shaped graph; and
- $\rho_i^{-1}(v_i)$ is an X-shaped graph.

Then $\partial X_i \setminus \text{Int}(\rho_i^{-1}(\partial P_i))$ consists of four disks $d_{i,1}$, $d_{i,2}$, $d_{i,3}$ and $d_{i,4}$, and the closure of $\rho_i^{-1}(\partial P_i) \setminus \text{Nbd}(\rho_i^{-1}(S(P)))$ consists of six squares $b_{i,1}, b_{i,2}, \dots, b_{i,6}$. We foliate each of these squares by intervals as shown in Figure 41. Set $W_i = X_i \times [-1, 1]$. We note

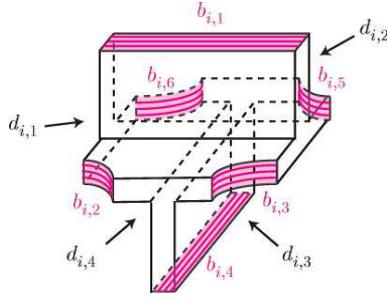


FIGURE 41. $P_i = \text{Nbd}(v_i; P)$.

that the 4-thickening W_0 of $\text{Nbd}(S(P); P)$, which is the subbundle of the determinant line bundle over X_i whose fiber is $[-1, 1]$ (after giving an Euclidean metric over this bundle), is obtained by gluing the pieces $W_1, W_2, \dots, W_{c(P)}$. Then the boundary ∂W of the 4-thickening W of P decomposes as:

$$W_i \cap \partial W = X_i \times \{-1\} \bigcup_{d_{i,j} \times \{-1\}} \left(\left(\bigcup_{i=1}^4 d_{i,j} \right) \times [-1, 1] \right) \bigcup_{d_{i,j} \times \{1\}} X_i \times \{1\}.$$

See Figure 42. In the figure, $d_{i,j} \times \{\pm 1\}$ ($j \in \{1, 2, 3, 4\}$) is denoted by $d_{i,j}^\pm$ and $b_{i,j} \times \{\pm 1\}$ ($j \in \{1, 2, \dots, 6\}$) is denoted by $b_{i,j}^\pm$. Moreover each $b_{i,j}^\pm$ inherits a foliation from $b_{i,j}$.

Let $X = \bigcup_{i=1}^{c(P)} X_i$ be the 3-dimensional thickening of $\text{Nbd}(S(P); P)$. Let $\rho \searrow \text{Nbd}(S(P); P)$ be the collapsing given by ρ_i ($i \in \{1, 2, \dots, c(P)\}$), and let $\pi : W_0 \searrow \text{Nbd}(S(P); P)$ be the collapsing given by ρ and the projection $[-1, 1] \rightarrow \{0\}$. Set $D_i = R_i \setminus \text{Int} \text{Nbd}(S(P), P)$ ($i \in \{1, 2, \dots, c(P)\}$). We note that P is obtained from $\text{Nbd}(S(P); P)$ by attaching each disk D_i along l_i . Suppose the boundary of the closure of R_i runs k_i times through the vertices of P . Then the preimage $\rho^{-1}(l_i)$, which is either an annulus or a Möbius band, is the union $\bigcup_{i=1}^{k_i} b_{\sigma(i), \tau(i)}$ with $\sigma(i) \in \{1, 2, \dots, c(P)\}$ and $\tau(i) \in \{1, 2, \dots, 6\}$. If $\rho^{-1}(l_i)$ is an annulus, it lies in the solid torus $\pi^{-1}(l_i)$ as shown in Figure 43. Then the annulus $\bigcup_{i=1}^{k_i} b_{\sigma(i), \tau(i)}$ is parallel to $\bigcup_{i=1}^{k_i} b_{\sigma(i), \tau(i)}^{\epsilon_i}$ in the solid torus $\pi^{-1}(l_i)$. Hence by the definition of gleams, attaching the disk D_i to P' along l_i and putting the gleam 0 on the resulting region R_i correspond to performing

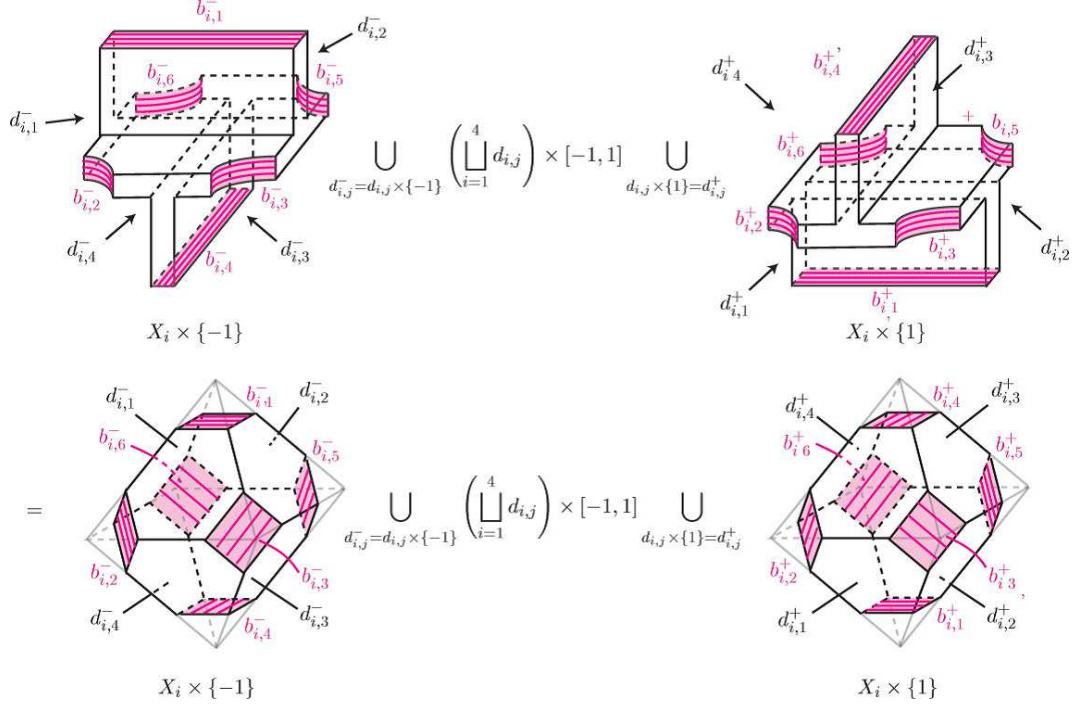


FIGURE 42. $W_i \cap \partial W$. Topologically, the part $(\prod_{i=1}^4 d_{i,j}) \times [-1, 1]$ can be ignored and we may regard $W_i \cap \partial W$ as two truncated octahedra $X_i \times \{\pm 1\}$ glued as $d_{i,j}^- = d_{i,j}^+$ ($j \in \{1, 2, 3, 4\}$).

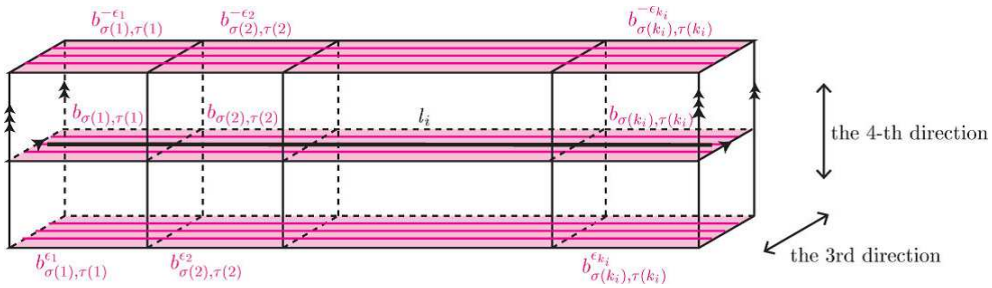


FIGURE 43. The solid torus $\pi^{-1}(l_i)$ in the case where $\rho^{-1}(l_i)$ is an annulus. In this figure, $\epsilon_i = \pm$.

Dehn filling on X along a leaf of the foliation on $\bigcup_{i=1}^{k_i} b_{\sigma(i),\tau(i)}^{\epsilon_i}$, which lies in the torus $T_i = \partial\pi^{-1}(l_i) \subset \partial X$. Moreover, putting the gleam $g_i \in \mathbb{Z}$ on R_i in this process corresponds to performing Dehn filling on X along the slope s_i obtained from the leaf by g_i -th power of the Dehn twist about the meridian of the solid torus $\pi^{-1}(l_i)$. Note that this slope s_i can be expressed by $g_i[\mu_i] + [\lambda_i] \in H_1(T_i; \mathbb{Z})$, where μ_i is a meridian of the solid

torus $\pi^{-1}(l_i)$ and λ_i is a leaf of the foliation on $\bigcup_{i=1}^{k_i} b_{\sigma(i),\tau(i)}^{\epsilon_i}$. If $\rho^{-1}(l_i)$ is a Möbius band, it lies in the solid torus $\pi^{-1}(l_i)$ as shown in Figure 44. In this case, the Möbius band

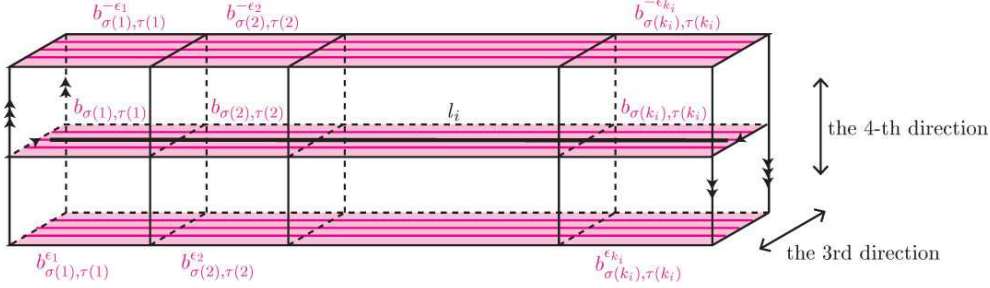


FIGURE 44. The solid torus $\pi^{-1}(l_i)$ in the case where $\rho^{-1}(l_i)$ is a Möbius band.

$\bigcup_{i=1}^{k_i} b_{\sigma(i),\tau(i)}$ is no longer parallel to the boundary of the solid torus $\pi^{-1}(l_i)$. Let $a_{\sigma(1),\tau(1)}^{\pm}$ be a foliated square shown in Figure 45. Then the union $a_{\sigma(1),\tau(1)}^{\pm} \cup (\bigcup_{i=2}^{k_i} b_{\sigma(i),\tau(i)})$ is

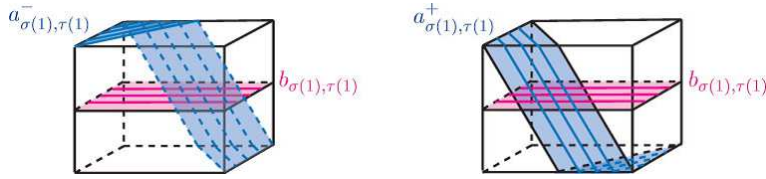


FIGURE 45. The foliation when the gleam is a half-integer.

an annulus that is isotopic to $\bigcup_{i=1}^{k_i} b_{\sigma(i),\tau(i)}^{\epsilon_i}$ after a $\pm 1/2$ -twist. Hence again by the definition of gleams, attaching the disk D_i to P' along l_i and putting the gleam $\pm 1/2$ on the resulting region R_i correspond to performing Dehn filling on X along a leaf of the foliation on $a_{\sigma(1),\tau(1)}^{\pm} \cup (\bigcup_{i=2}^{k_i} b_{\sigma(i),\tau(i)})$. Moreover, putting the gleam $g_i \in (\frac{1}{2}\mathbb{Z}) \setminus \mathbb{Z}$ on R_i in this process corresponds to performing Dehn filling on X along the slope s_i obtained from a leaf of $a_{\sigma(1),\tau(1)}^{+} \cup (\bigcup_{i=2}^{k_i} b_{\sigma(i),\tau(i)})$ by $(g_i - 1/2)$ -th power of Dehn twist about the meridian of the solid torus $\pi^{-1}(l_i)$. Again, note that this slope s_i can be written as $(g_i - 1/2)[\mu_i] + [\lambda_i] \in H_1(T_i; \mathbb{Z})$, where μ_i is a meridian of the solid torus $\pi^{-1}(l_i)$ and λ_i is a leaf of the foliation on $a_{\sigma(1),\tau(1)}^{+} \cup (\bigcup_{i=2}^{k_i} b_{\sigma(i),\tau(i)})$.

As is explained in [12], we can equip the interior of X with a complete, finite volume hyperbolic structure by regarding X as $2c(P)$ regular ideal octahedra glued by isometries. The decomposition of the interior of X into these ideal octahedra exactly corresponds to the decomposition described in Figure 42. We recall that the regular ideal octahedron has a maximal horocusp section consisting of six Euclidean unit squares. This maximal horocusp gives rise to a maximal horoball neighborhood C of the interior of X . By the above argument, the length of the slope s_i with respect to C coincides with $\text{sl}(R_i)$. \square

ACKNOWLEDGMENTS

The authors wish to express their gratitude to Francesco Costantino, Bruno Martelli and Osamu Saeki for very helpful suggestions and comments. This work was carried out while the second-named author was visiting Università di Pisa as a JSPS Postdoctoral Fellow for Reserch Abroad. He is grateful to the university and its staffs for the warm hospitality.

REFERENCES

- [1] Agol, I., Lower bounds on volumes of hyperbolic Haken 3-manifolds, arXiv:math/9906182.
- [2] Agol, I., Bounds on exceptional Dehn filling, *Geom. Topol.* **4** (2000), 431–449.
- [3] Agol, I., Storm, P. A., Thurston, W. P., Lower bounds on volumes of hyperbolic Haken 3-manifolds. With an appendix by Nathan Dunfield, *J. Amer. Math. Soc.* **20** (2007), 1053–1077.
- [4] Benedetti, R., Petronio, C., *Branched standard spines of 3-manifolds*, Lecture Notes in Mathematics **1653**, Springer-Verlag, Berlin, 1997.
- [5] Burlet, O., de Rham, G., Sur certaines applications génériques d’une variété close à 3 dimensions dans le plan, *Enseignement Math. (2)* **20** (1974), 275–292.
- [6] Callahan, P. J., Dean, J. C., Weeks, J. R., The simplest hyperbolic knots, *J. Knot Theory Ramifications* **8** (1999) 279–297.
- [7] Costantino, F., *Shadows and branched shadows of 3 and 4-manifolds*, Edizioni della Normale, Scuola Normale Superiore, Pisa, Italy, 2005.
- [8] Costantino, F., A short introduction to shadows of 4-manifolds, *Fund. Math.* **188** (2005), 271–291.
- [9] Costantino, F., Stein domains and branched shadows of 4-manifolds, *Geom. Dedicata* **121** (2006), 89–111.
- [10] Costantino, F., Branched shadows and complex structures of 4-manifolds, *J. Knot Theory Ramifications* **17** (2008), 1429–1454.
- [11] Costantino, F., Frigerio, R., Martelli, B., Petronio, C., Triangulations of 3-manifolds, hyperbolic relative handlebodies, and Dehn filling, *Comment. Math. Helv.* **82** (2007), 903–933.
- [12] Costantino, F., Thurston, D., 3-manifolds efficiently bound 4-manifolds, *J. Topol.* **1** (2008), 703–745.
- [13] Endoh, M., Ishii, I., A new complexity for 3-manifolds, *Japan. J. Math. (N.S.)* **31** (2005), 131–156.
- [14] Futer, D., Kalfagianni, E., Purcell, J. S., Dehn filling, volume, and the Jones polynomial, *J. Differential Geom.* **78** (2008), 429–464.
- [15] Gromov, M., Singularities, expanders and topology of maps. I. Homology versus volume in the spaces of cycles, *Geom. Funct. Anal.* **19** (2009), 743–841.
- [16] Ikeda, H., Acyclic fake surfaces, *Topology* **10** (1971), 9–36.
- [17] Ishii, I., Flows and spines, *Tokyo J. Math.* **9** (1986), 505–525.
- [18] Kalmár, B., Stipsicz, A. I., Maps on 3-manifolds given by surgery, *Pacific J. Math.* **257** (2012), 9–35.
- [19] Kapovich, M., *Hyperbolic manifolds and discrete groups*, Progress in Mathematics **183**, Birkhäuser Boston Inc., Boston, MA, 2001.
- [20] Koda, Y., Branched spines and Heegaard genus of 3-manifolds, *Manuscripta Math.* **123** (2007), 285–299.
- [21] Kushner, L., Levine, H., Porto, P., Mapping three-manifolds into the plane. I, *Bol. Soc. Mat. Mexicana (2)* **29** (1984), 11–33.
- [22] Lackenby, M., Word hyperbolic Dehn surgery, *Invent. Math.* **140** (2000), 243–282.
- [23] Levine, H., Elimination of cusps, *Topology* **3** (1965), 263–296.
- [24] Levine, H., *Classifying immersions into \mathbb{R}^4 over stable maps of 3-manifolds into \mathbb{R}^2* , Lecture Notes in Mathematics **1157**, Springer-Verlag, Berlin, 1985.

- [25] Martelli, B., Links, two-handles, and four-manifolds, *Int. Math. Res. Not. IMRN* **2005**, 3595–3623.
- [26] Martelli, B., Four-manifolds with shadow-complexity zero, *Int. Math. Res. Not. IMRN* **2011**, 1268–1351.
- [27] Matveev, S. V., *Algorithmic Topology and Classification of 3-Manifolds*, Algorithms Comput. Math. **9**, Springer, Berlin, 2003.
- [28] Morgan, J. W., On Thurston’s uniformization theorem for three-dimensional manifolds, *The Smith conjecture (New York, 1979)*, pp. 37–125, Pure Appl. Math. **112**, Academic Press, Orlando, FL, 1984.
- [29] Otal, J-P., *Le théorème d’hyperbolisation pour les variétés fibrées de dimension 3*, *Astérisque* **235**, 1996.
- [30] Otal, J-P., Thurston’s hyperbolization of Haken manifolds, *Surveys in differential geometry, Vol. III (Cambridge, MA, 1996)*, pp. 77–194, Int. Press, Boston, MA, 1998.
- [31] Perelman, G., The entropy formula for the Ricci flow and its geometric applications, arXiv:math/0211159.
- [32] Perelman, G., Ricci flow with surgery on three-manifolds, arXiv:math/0303109.
- [33] Perelman, G., Finite extinction time for the solutions to the Ricci flow on certain three-manifolds, arXiv:math/0307245.
- [34] Petronio, C., Generic flows on 3-manifolds, arXiv:1211.6445.
- [35] Rolfsen, D., *Knots and links*, Mathematics Lecture Series **7**, Publish or Perish, Inc., Berkeley, Calif., 1976.
- [36] Saeki, O., Simple stable maps of 3-manifolds into surfaces, *Topology* **35** (1996), 671–698.
- [37] Saeki, O., *Topology of singular fibers of differentiable maps*, Lecture Notes in Mathematics **1854**, Springer-Verlag, Berlin, 2004.
- [38] Thurston, D., The algebra of knotted trivalent graphs and Turaev’s shadow world, *Invariants of knots and 3-manifolds (Kyoto, 2001)*, pp. 337–362, *Geom. Topol. Monogr.* **4**, Geom. Topol. Publ., Coventry, 2002.
- [39] Thurston, W. P., *The geometry and topology of three-manifolds*, lecture notes, Princeton University, Princeton, 1980, available at <http://msri.org/publications/books/gt3m/>.
- [40] Thurston, W. P., Three-dimensional manifolds, Kleinian groups and hyperbolic geometry, *Bull. Amer. Math. Soc. (N.S.)* **6** (1982), 357–381.
- [41] Turaev, V. G., Shadow links and face models of statistical mechanics, *J. Differential Geom.* **36** (1992), 35–74.
- [42] Turaev, V. G., *Quantum invariants of knots and 3-manifolds*, de Gruyter Studies in Mathematics **18**, Walter de Gruyter & Co., Berlin, 1994.
- [43] Yoshida, K., The minimal volume orientable hyperbolic 3-manifold with 4 cusps, arXiv:1209.1374.

TOHOKU UNIVERSITY, SENDAI, 980-8578, JAPAN
E-mail address: ishikawa@m.tohoku.ac.jp

MATHEMATICAL INSTITUTE
 TOHOKU UNIVERSITY, SENDAI, 980-8578, JAPAN
 AND
 (TEMPORARY) DIPARTIMENTO DI MATEMATICA
 UNIVERSITÀ DI PISA, LARGO BRUNO PONTECORVO 5, 56127 PISA, ITALY
E-mail address: koda@math.tohoku.ac.jp